Office of Naval Research

Contract N50RI-76 • Task Order No.1 • NR-078-011

FULL-WAVE DETECTION OF SIGNALS IN NOISE

By

Noel Stone and David Middleton

August 1, 1953

Technical Report No. 182

Cruft Laboratory
Harvard University
Cambridge, Massachusetts

Office of Naval Research

Contract N5ori-76

Task Order No. 1

NR-078-011

Technical Report

on

Full-Wave Detection of Signals in Noise

by

Noel Stone and David Middleton

August 1, 1953

The research reported in this document was made possible through support extended Cruft Laboratory, Harvard University, jointly by the Navy Department (Office of Naval Research), the Signal Corps, of the U. S. Army, and the U. S. Air Force under CNR Contract N5ori-76, T. O. 1.

Technical Report No. 182

Cruft Laboratory

Harvard University

Cambridge, Massachusetts

CONTENTS

FIGURES

ABSTRACT

The experimental background for the theoretical problems to be investigated is first reviewed, and then a brief sketch of the classical detection problem is included. A signal-to-noise ratio is defined, and the principle results of the study are summarized and discussed in some detail, with the important quantities in the derivation of the output signal-to-noise ratio after full-wave rectification, for input background noise of gaussian statistics, being obtained from the correlation function for the output. The cases treated are: 1(a) a sinusoidal signal in narrow-band noise, 1(b) a narrow-band noise "signal" in a narrow-band noise background, 2(a) a sinusoidal signal in broad-band noise, 2(b) a narrow-band noise "signal" in a broad-band noise background. The half-wave and full-wave cases are compared. The important devices, the ideal clipper, linear detector, and square-law detector, are considered, and compared for the extremes of very large and very small input signal-to-noise ratios. Thus, for all varieties of input outlined above if p is the input power signal-to-noise ratio, then for very small p, the output power signal-to-noise ratio, P, is related to p by $P \sim p^2$, for all devices. For sinusoidal signals (large p) and linear and quadratic detectors, P is proportional to p, whereas for the ideal clipper, $P \sim (\ln p)^2 p$. The exact relations are summarized in Part I, sec. 4 of this report.

TR182

FULL-WAVE DETECTION OF SIGNALS IN NOISE

by

Noel Stone and David Middleton

Cruft Laboratory, Harvard University

Cambridge, Massachusetts

I

Introduction and Results

1. The Experimental Background

Before we consider the theoretical aspects of the problems examined here, it is necessary to review the experimental situation which serves as background for this discussion. Most of the applications of our results are of interest when applied to the problems involved in the passive detector case; i.e., the situation wherein the receiver has no control over the signal being detected, and only a certain limited amount of information about its characteristics.

We distinguish first between:

1(a) the case where the specific (fundamental) frequency of the signal, f_o, is known, if the signal is periodic,

1(b) the bandwidth, B, and mean frequency, f_o, are known, if the signal is random,

2(a) the specific (fundamental) frequency of the signal, f_o, is known to lie in a certain band of frequencies, if the signal is periodic, the exact location of f_o being unknown,

2(b) f_o is known to lie in a certain band of frequencies, if the signal is random, the exact location of f_o being unknown.

In all these instances the signal is masked by noise.

In practice, case 1(a) occurs when the receiver is searching for a source which is emitting a known signal, e.g., as in certain radar, radio, underwater sound, or radio-astronomy situations. In all these cases, the

frequency is known a priori from other considerations. However, in case 2 (a) above, we have a state of less information, where the specific frequency of the sources is not known. Spectrally, we may describe the situation schematically as in Fig. 1.

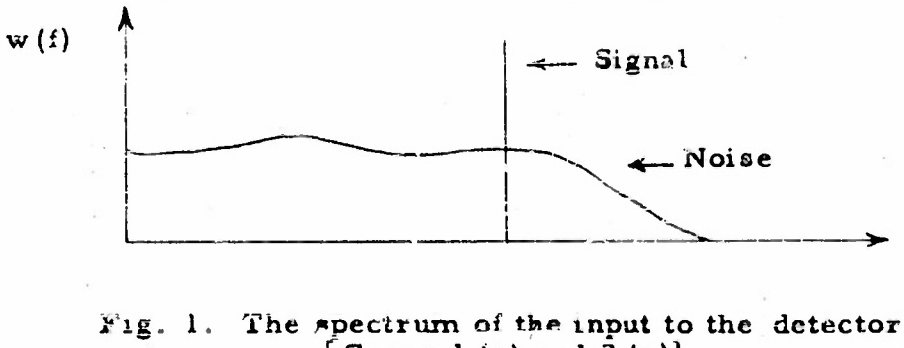

Fig. 1. The spectrum of the input to the detector [Cases 1 (a) and 2 (a)]

Here, w(f) is the power spectrum of the wave at the receiver's input. The experimental situations corresponding to 1 (b) and 2 (b) may involve a detector observing an infra-red source which has an appreciable continuous spectrum in some frequency region; a water-borne sound signal of a random character, or astronomical noise from some region of the night sky, etc. In such instances we may frequently represent the random "signal" as having a spectral shape of the type shown in Fig. 2 below.

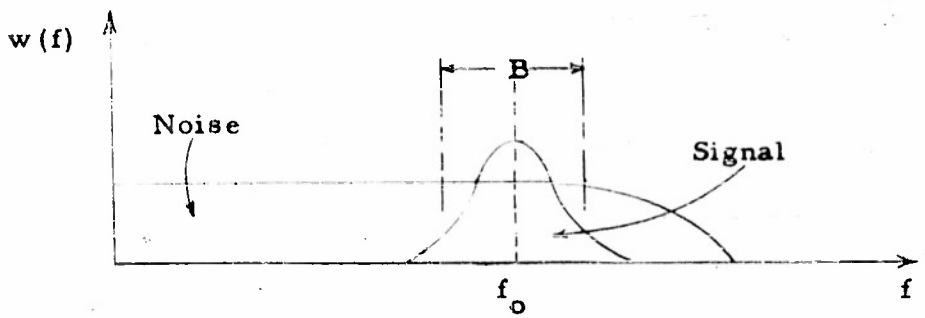

Fig. 2. The spectrum of the input to the detector [Cases 1 (b) and 2 (b)]

As before, case 1 (b) is distinguished from case 2 (b) by the fact that the central frequency, f_o, and bandwidth, B, are not precisely known in the

latter.

In case 1(a) it is clear that improvement in detection results, as is well known, when a suitable narrow-band pre-detection filter is located about the frequency f_o, as shown in Fig. 3.

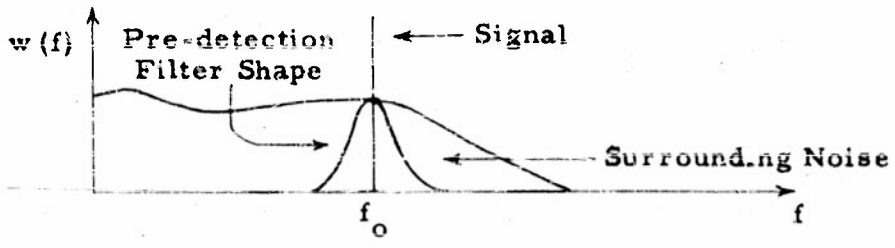

Fig. 3. An example of pre-detection filtering, case 1(a).

In this case, the narrower this filter, the greater the reduction in input noise. A similar circumstance arises in case 1(b). The appropriate pre-detection filter here has a finite bandwidth, depending on the signal structure and the character of the noise.[1-4] If the noise is broad-band, then the optimum filter has a frequency response, for example, which is the conjugate image of the amplitude spectrum of the signal. If the noise lies in a band narrower than the signal, the signal spectrum being $S(f)$, and the intensity spectrum of the noise $N(f)$, then the optimum pre-detection filter, $H(f)$, will be one for which

$$H(f) = \lambda S(f)^* / N(f),$$

where λ is an appropriate constant.

Therefore we have to consider the following models of the input to the detector:

1(a) a sinusoidal signal in narrow-band noise.

1(b) a narrow-band (gaussian) noise "signal" in narrow-band noise.

2(a) a sinusoidal signal in broad-band noise.

2(b) a narrow-band noise "signal" in broad-band noise.

Each of these corresponds to the detection situation previously outlined, with the appropriate pre-detection filtering. Apart from the specific situations mentioned above, it is also clear that the analysis can be applied to any prob-

lem for which these models are representative.

2. The Detection Process.

Let us now review some of the principal features of the detection process itself, as illustrated for sinusoidal input by the procedure shown in Fig. 4 below.

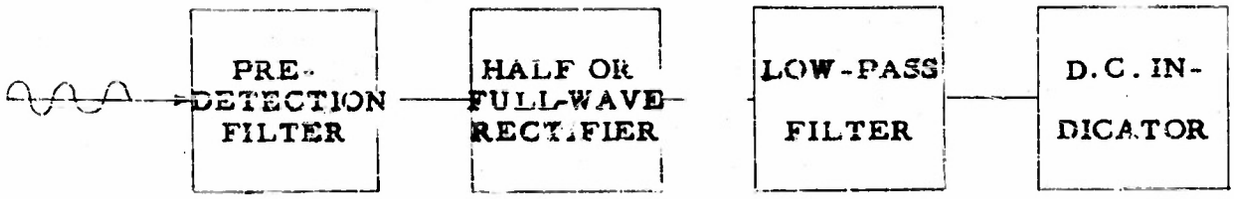

Fig. 4. A typical detection scheme for a sinusoidal signal.

The half or full-wave rectifiers are usually linear or quadratic. The scheme of Fig. 4 can be represented spectrally in the manner of Fig. 5, the fundamental frequency in the output being twice that of the input for the full-wave case. The low-frequency, low-pass filter (cf. Fig. 4) is designed to eliminate the harmonics, and admit only the direct current to

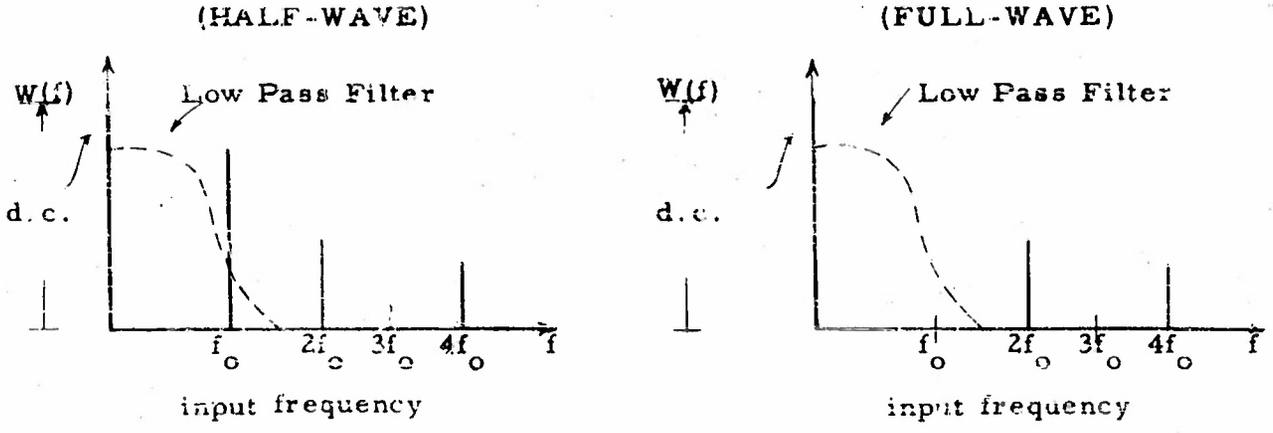

Fig. 5. Spectrum of the output following half- or full-wave rectification for a sinusoidal input of frequency f_o.

the indicator. (The spectral lines here are simply the squares of the absolute values of the Fourier components of the output.) These are obtained from a knowledge of:

(1) the nature of the input
(2) the character of the nonlinear device
(3) the resulting output time function
(4) the decomposition of the output into a Fourier series (or Fourier integral).

A similar operation is required in the more general circumstance where random processes are involved. Here, instead of a sine input, we might introduce, for example, narrow-band noise centered on f_o into either the half- or full-wave device. The output spectrum has a zonal distribution (sec. 3, ref. 5) at harmonics of the fundamental, or twice its frequency. However, a low-pass filter removing the higher harmonic zones now includes a part of

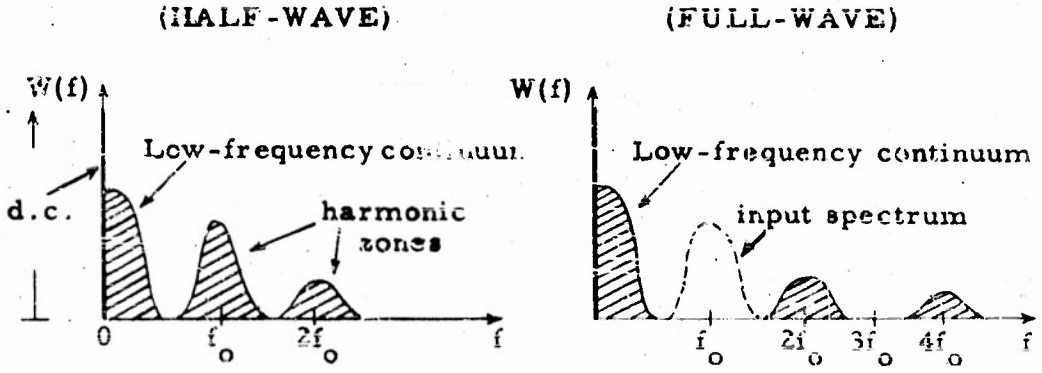

Fig. 6. Typical spectra of the output following half- or full-wave rectification of a narrow-band noise input.

the input noise spectrum; namely, part of the low-frequency continuum. Thus, the d-c indicator responds not only to the direct current, but to an accompanying noise wave as well, which acts to obscure the true d-c reading. The part of the low-frequency continuum which is passed by the low-pass filter we shall call here "fluctuation noise." The situation is illustrated in Fig. 7. Here, $W(f)_o$ represents the low-frequency continuum. The fluctuation noise power, N^2, is

$$N^2 = \int_0^\infty |H(f)|^2 \, W(f)_o \, df, \qquad (2.1)$$

where $|H(0)| = 1$.

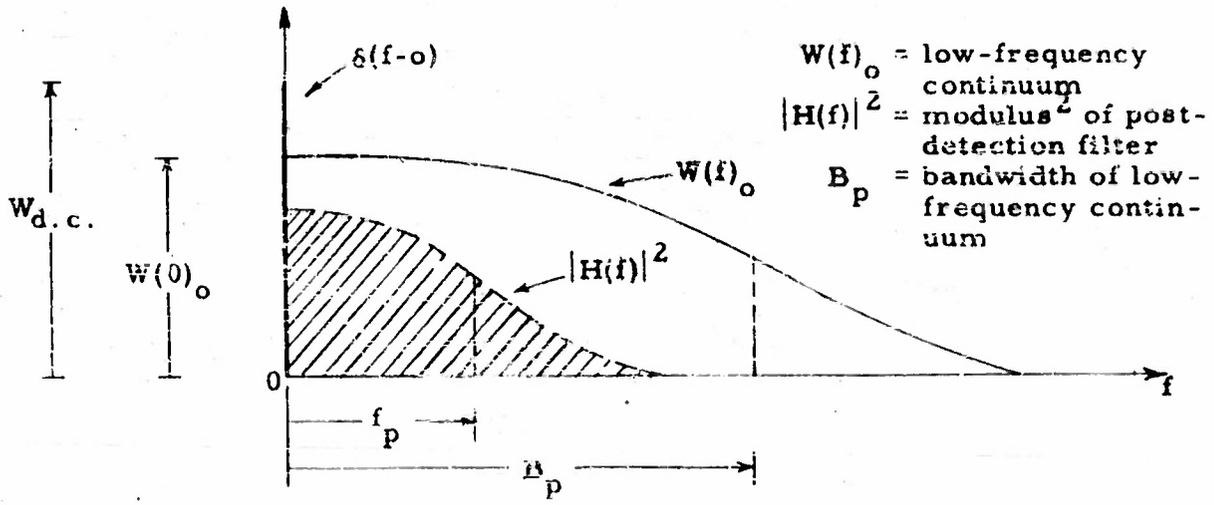

Fig. 7. A spectrum of fluctuation noise accompanying a d-c reading after detection of an input noise wave.

Since a physically realizable filter must have finite bandwidth (or equivalently, finite response time), a portion of the low-frequency continuum is always retained in the indication, and a fluctuation noise of rms deviation N is always present in the d-c reading. Referring to Fig. 7, if the post-detection bandwidth f_p* is very small compared to B_p*, we observe then that the low-frequency continuum is essentially constant and equal to $W(0)_o$ over the frequency range where $|H(f)|$ has an appreciable value. Therefore, we are justified in writing, for this case,

$$N^2 \equiv W(0)_o \int_o^\infty |H(f)|^2 \, df. \qquad (2.2)$$

In the equivalent rectangular (ideal) filter, where

$$|H(f)|^2 = 1 \qquad 0 \leqslant f < fp \qquad (2.3)$$
$$= 0 \qquad fp < f$$

*Here, the frequency at which $W(f)_o$ is one half the maximum spectral intensity, $W(0)_o$.

the noise intensity is

$$N^2 = W(0)_o f_p . \tag{2.4}$$

For a post-detection filter of a shape different from the ideal, we have

$$N^2 = kW(0)_o f_p . \tag{2.5}$$

Basic to all these expressions is the assumption that the observation time is infinite, even though the response time of the filter may be finite. [For a more detailed discussion of the measuring process, taking into account finite averaging time, cf. forthcoming report by J. Storer and D. Middleton].

When a signal is included with the noise, and the signal is a sine wave, then in addition to the above low-frequency continuum, which represents (noise×noise) noise components (ref. 5, sec. 3), the noise also interacts with the signal to produce (signal×noise) noise terms which make additional contributions to the low-frequency fluctuation.

3. The Signal-to-Noise Ratio as a Detection Criterion.

Criteria may be set up, for the performance of a detection system, of the sort shown in Fig. 4. Given at the input a certain signal-to-noise ratio, we wish to determine the signal-to-noise ratio after the nonlinear operation and filtering. A useful (though limited) definition of what constitutes a signal in the output may be constructed as follows: we observe first that the nonlinear operation has converted the input into an output indication, appearing on some essentially d-c indicator. If the signal is presented as an on-off indication (and such a signal might appear at a directional receiving element when steering onto the signal source) then these is a certain increment in this d-c reading due to the presence of the signal, as compared to the reading for noise alone. (We assume here an ever-present noise background). This increment in the amplitude of the deflecting needle (or whatever indicator is used) we define as our signal (regardless of the units in which it happens to be measured). The accompanying fluctuation noise constitutes the interference at the output; its observing effect we shall indicate by an rms amplitude.

Then, letting F = output signal-to-noise intensity ratio, ($\sqrt{F}$ = amplitude

ratio), and $(W_{d.c.})_{S+N}$, $(W_{d.c.})_N$, and $(N^2)_{S+N}$ be respectively the output d-c intensity with signal and noise; the output d-c intensity with noise alone; and the intensity of the fluctuation noise, we can write for the amplitude of the signal increment,

$$S = \sqrt{(W_{d.c.})_{S+N}} - \sqrt{(W_{d.c.})_N} ,$$

so that, for our (amplitude) ratio at the output:

$$\left(\frac{S}{N}\right)_{out} = \sqrt{P} = \sqrt{(W_{d.c.})_{S+N}} - \sqrt{(W_{d.c.})_N} \Big/ \sqrt{(N^2)_{S+N}} . \quad (3.1)$$

For an ideal filter, the noise admitted in post-detection, N_I^2, is from (2.4)

$$N_I^2 = W(0)_o (f_p)_I , \quad (3.2)$$

where $(f_p)_I$ refers to the bandwidth of the ideal filter as defined in equation (2.3). For a physically realizable filter of bandwidth $(f_p)_R$ as normally defined (cf. p. 6, footnote), we see that the post-detection fluctuation noise through this filter is

$$N_R^2 = W(0)_o \int_o^\infty |H(f)|^2 \, df \quad (3.3)$$

$$= k\, W(0)_o (f_p)_R .$$

Final results are expressed in terms of the bandwidth of the ideal filter, $(f_p)_I$, so that a relation is desired between $(f_p)_I$ and $(f_p)_R$. Comparing filters which pass the same amount of fluctuation noise, we set

$$N_I^2 = N_R^2$$

and then

$$(f_p)_I = k\,(f_p)_R . \quad (3.4)$$

For example, let us consider an RC combination as shown in Fig. 8. The function $|H(f)|^2$ is given by

$$|H(f)|^2 = \left|\frac{V_c}{V}\right|^2 = \frac{\beta^2}{\beta^2+\omega^2} \quad , \quad \beta = \frac{1}{RC} \tag{3.5}$$

$$(f_p)_R = \frac{\beta}{2\pi} = \frac{1}{2\pi RC} ,$$

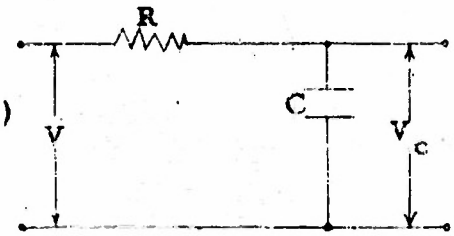

Fig. 8. Typical post-detection averaging circuit.

and

$$(f_p)_I = \int_0^\infty |H(f)|^2 \, df = \frac{\beta}{4} = \frac{\pi}{2}(f_p)_R \ , \tag{3.6}$$

so that $k = \frac{\pi}{2}$ for this actually realizable type of post-detection filtering. In all subsequent work f_p is written wherever $(f_p)_I$ should appear, an ideal filter being assumed. As for (2.4), we accordingly write

$$N^2_{S+N} = W(0)_o f_p \ . \tag{3.7}$$

Any conversion to other filters may be accomplished with (3.4).

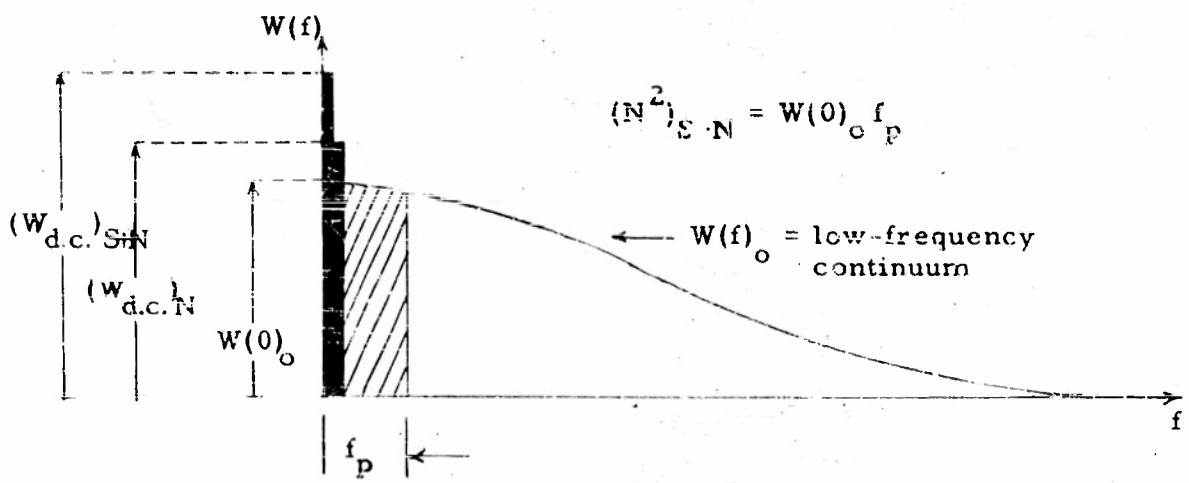

Fig. 9. Quantities determining output (S/N) ratio.

For the ideal filter, from (2.4) the output fluctuation noise is represented by the total area of the vertical, shaded strip. Thus, it is necessary to

determine the spectral intensity after detection, $W(0)_o$, for all cases, $(W_{d.c.})_{S+N}$, and $(W_{d.c.})_N$. The calculations follow the schema (1) - (4), p. 5, for the case of a purely sinusoidal signal alone, except that in step 4 we now require:

(4) the power spectrum $W(f)$ of the output; which is most conveniently determined here from the auto-correlation function, $R(t)$, of the rectified wave, with the aid of the well-known theorem of Weiner and Khintchine,[6,7]

$$W(f) = 4\int_o^\infty R(t)\cos\omega t\, dt \quad ; \quad \omega = 2\pi f \tag{3.8}$$

$$R(t) = \int_o^\infty W(f)\cos\omega t\, df \quad .$$

Before the analysis can be made, we must specify the nonlinear device to be used in detection. In our treatment we assume a ν-th law device; i.e., if x is the (instantaneous) input and y the corresponding (instantaneous) output, then

$$y = \beta|x|^2 \qquad (-\infty < x < \infty) \tag{3.9}$$

for the full-wave device, and for the half-wave rectifier,

$$\begin{aligned} y &= \beta x^2 && x \geq 0 \\ &= 0 && x < 0 \quad . \end{aligned} \tag{3.10}$$

A useful variety of devices may be represented by these relations, (3.9-10), as sketched in Fig. 10. Thus $\nu = 1,2$ represent the familiar "linear" and quadratic detectors; very small ν provides a model of rectification with saturation and large values of ν, the response of a crystal over a useful range. [A limitation of this characterization is that an additional arbitrary parameter, representing saturation, is not included, which may make it difficult to fit to an actual dynamic response over the entire range. This, however, presents no problem in the derivation of the desired output correlation function,

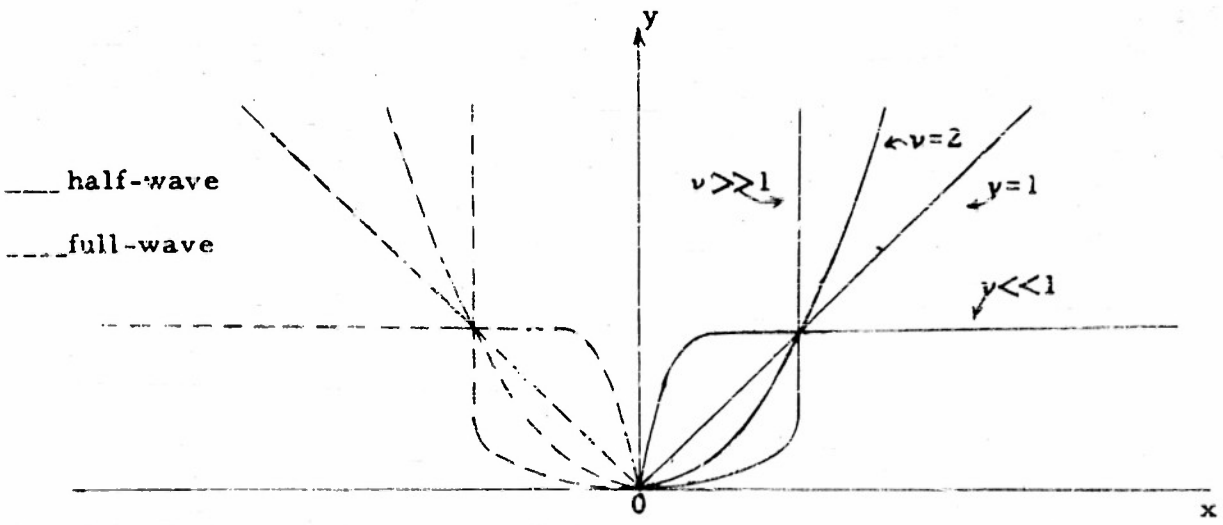

Fig. 10. The general half- and full-wave νth-law device.

from which we obtain the various spectra and powers.)

4. Discussion of the Results.

Let us now summarize the results of the present study. We have the following notation:

(1) p = input s/n power ratio
(2) f_F = pre-detection noise bandwidth
(3) f_p = post-detection filter bandwidth
(4) ν = power law of the nonlinear device
(5) P = output S/N power ratio

Then, when $p \ll 1$, [cf. eqs. (8.9b)]

$$\left(\frac{2}{\pi}\right)\left(\frac{\omega_P}{\omega_F}\right) P_{N.B.} \simeq Q_1(\nu)\, p^2 \tag{4.1}$$

for both sinusoidal and narrow-band noise signals in a narrow-band noise background, where Q_1 possesses a maximum at $\nu = 2$, and is precisely represented in Fig. 12. It is assumed that the input, narrow-band noise has an "optical" (i.e. single-tuned) normalized spectrum, $w(f)$, given by[8]

$$w(f) = \frac{2}{\pi} \frac{f_F}{f_F^2 + 4(f - f_o)^2} \quad * \qquad (4.2)$$

$$\int_o^\infty w(f)\, df = 1 \quad , \qquad f_o \gg \frac{\beta}{2\pi} \quad .$$

For a sine-wave in a broad-band noise background, when $p \ll 1$, a similar law holds [cf. eqs. (10.23) and (10.24)]

$$\left(\frac{2}{\pi}\right)\left(\frac{\omega p}{\omega_F}\right) P_{B.B.} \simeq Q_2(\nu)\, p^2 \quad , \qquad (4.3)$$

where $Q_2(\nu)$ has a behavior similar to Q_1, as shown in Figs. 13 and 14. The broad-band noise is described by a normalized optical spectrum[8]:

$$w(f)_o = \frac{4}{\pi} \frac{(f_F)_o}{(f_F)_o^2 + f^2} \quad , \qquad (**)(4.4)$$

or by a normalized Gauss spectrum:[8]

$$w(f)_G = \frac{2\sqrt{\pi}}{a}\, e^{-\frac{\omega^2}{4a^2}} \quad ; \quad a^2 = \left(\frac{-\ln 1/2}{\pi}\right)(f_F)_G^2 \quad . \qquad (**)(4.5)$$

These are the spectra covered by Figs. 13 and 14 respectively. When both broad-band spectra (4.4) and (4.5) represent the same input noise power, the following relation holds between their bandwidths:

$$(f_F)_G = \sqrt{\pi}\, (f_F)_o \quad . \qquad (4.6)$$

In both of equations (4.1) and (4.3) the striking feature to note is the modulation suppression effect[2,9] whereby the output ratio is proportional to the

---

*where f_F is the frequency interval between half-power points relative to max. $w(f)$ at $f = f_o$.

**Both $(f_F)_o$ and $(f_F)_G$ represent the frequency interval between the half-power point and the max. $w(f)$ at $f = 0$.

square of input ratio for threshold signals.

We next ask how the output depends on the law of the detector. Examination of ν-dependent factors shows that, for both detection schemes [1(a), 1(b)] and 2(a) the quadratic detector ($\nu = 2$) yields a maximum for Ω_1 and Ω_2. These factors exhibit the general behavior sketched in Fig. 11 (for comparison), the exact forms being given in Figs. 12-14.

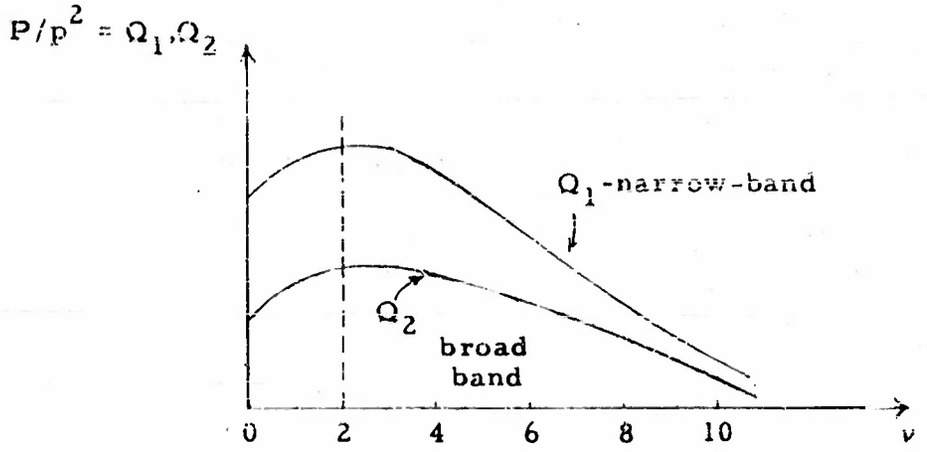

Fig. 11. Small signal variation of P/p^2 for various devices and detection schemes.

It is clear that P depends on both ν and p. The above remarks suggest a way in which the results may conveniently be presented: we observe that the behavior of a particular ν-th law device over the entire range of input (s/n) values is described if P is given as a function of p, with ν as parameter. Alternatively, if it is known at the detector that the input signal has a certain value of p, and a device is desired which yields a suitable value of P (usually the maximum), then P is expressed as a function of ν, with p as parameter.)

Further insight into the operation of these detection schemes for weak signals may be obtained from (4.1) and (4.3). Let us compare values of P for a sinusoidal signal in broad-band noise and in narrow-band noise, when a signal of power level σ is received through a broad-band channel of width $(f_F)_{B.B.}$, and of a mean intensity per cycle μ, defined by

$$\mu_{B.B.} = \int_0^\infty \frac{w(f)_{B.B.}}{(f_F)_{B.B.}}\, df \qquad (4.7)$$

and when the same signal is received through a narrow-band channel of width $(f_F)_{N.B.}$, and mean intensity per cycle, $\mu_{N.B.}$ defined by

$$\mu_{N.B.} = \int_0^\infty w(f)_{N.B.}\, df \Big/ (f_F)_{N.B.} \quad , \tag{4.8}$$

with the same post-detection bandwidth f_p in both cases. If the mean intensity per cycle for both noise backgrounds is the same, then the output power $(P = (S/N)^2)$ ratios in both instances are

$$P_{N.B.} = \left[\frac{\pi}{f_p}\left(\frac{\sigma}{\mu}\right)^2\right] \frac{Q_1}{(f_F)_{N.B.}} \quad , \tag{4.9}$$

and

$$P_{B.B.} = \left[\frac{\pi}{f_p}\left(\frac{\sigma}{\mu}\right)^2\right] \frac{Q_2}{(f_F)_{B.B.}} \tag{4.10}$$

where we have set

$$\mu = \mu_{B.B.} = \mu_{N.B.} \quad , \tag{4.11}$$

$$P_{N.B.} = \mu (f_F)_{N.B.}$$

$$P_{B.B.} = \mu (f_F)_{B.B.} \quad .$$

Therefore, the gain G(db) of $P_{N.B.}$ over $P_{B.B.}$ may be expressed as

$$G = 10 \log_{10}\left[\frac{P_{N.B.}}{P_{B.B.}}\right] = 10 \log_{10}\left(\frac{Q_1}{Q_2}\right) + 10 \log_{10}\left[\frac{(f_F)_{B.B.}}{(f_F)_{N.B.}}\right]. \tag{4.12}$$

The factor (Q_1/Q_2) arises from the fact that no low-frequency fluctuation noise appears at the input for narrow-band noise, as is not the case for broad-band noise. Thus, if a broad-band detection scheme were in force, but it was known that the signals did not lie in the band f_p, there would be an intrinsic gain of $10 \log_{10}(Q_1/Q_2)$ in P, from the fact that this small band of noise at the input does not appear. The quantity Q_1/Q_2 is plotted in Fig. 16 for a

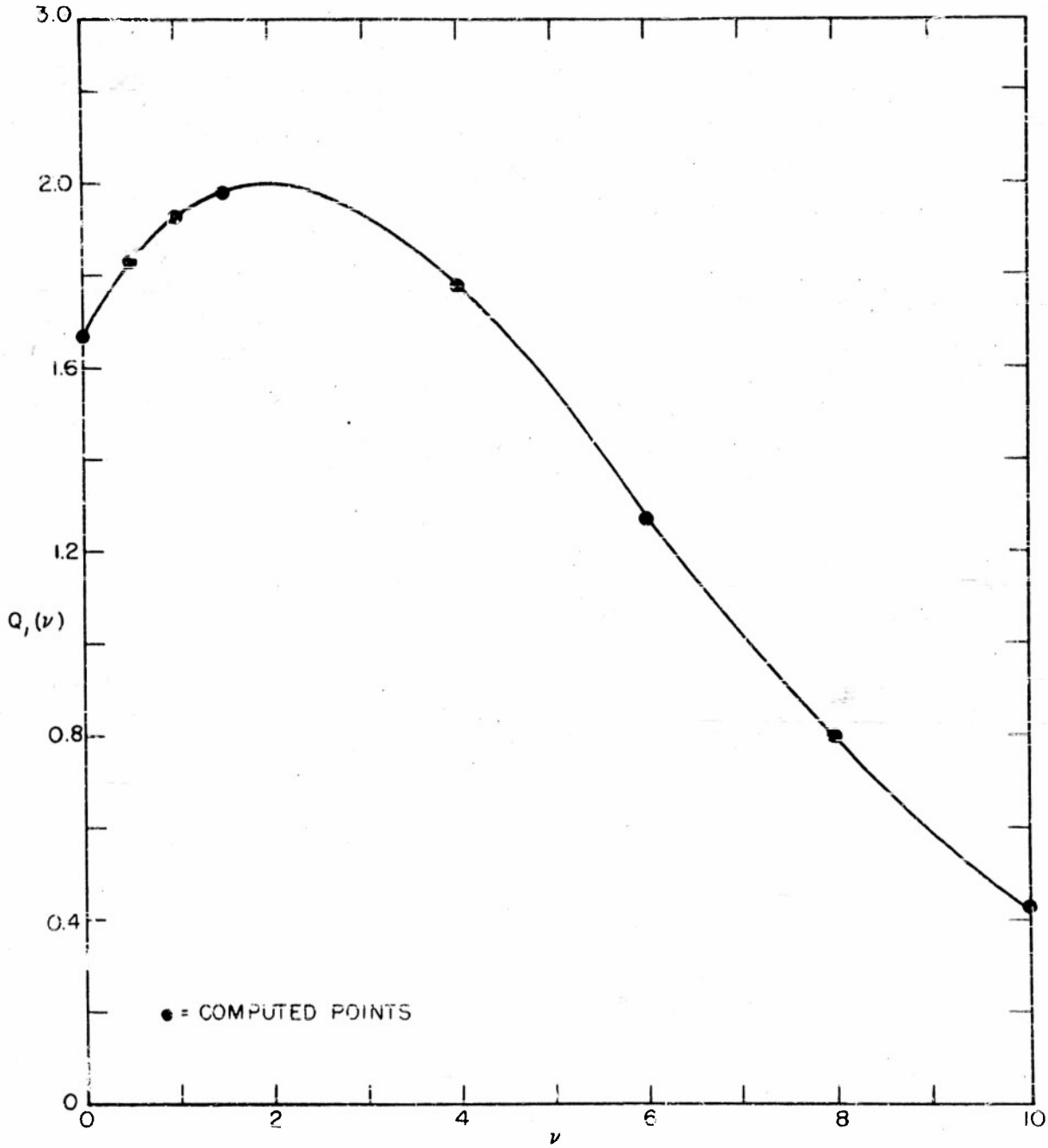

FIG. 12a $Q_1(\nu): P/p^2$ FOR WEAK INPUT SIGNALS. INPUT: SINEWAVE OR NARROW-BAND "OPTICAL" (SINGLE-TUNED) NOISY "SIGNAL", IN NARROW-BAND "OPTICAL" NOISE.

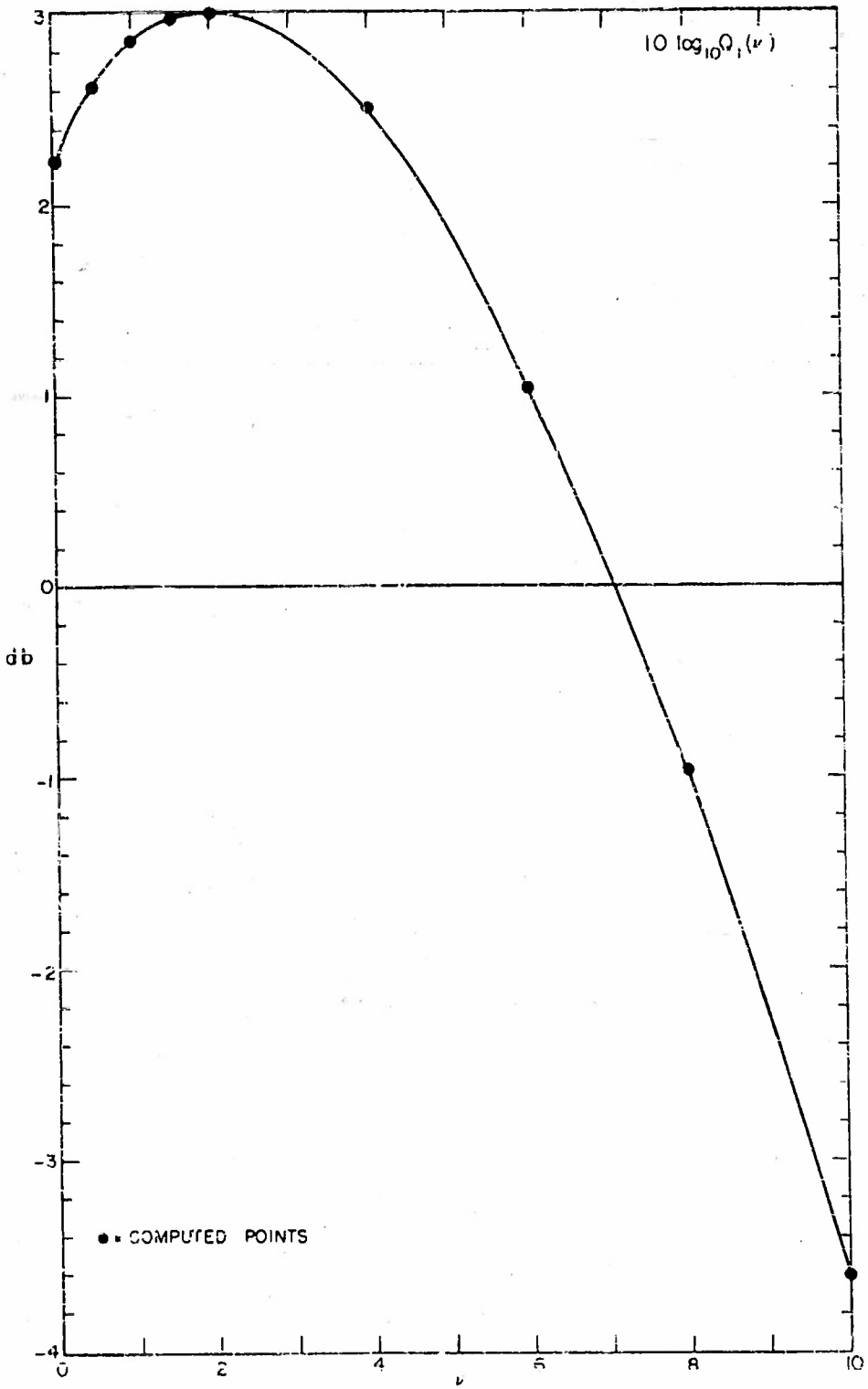

FIG. 12b 10 $\log_{10} Q_1(\nu)$; P/p^2 FOR WEAK INPUT SIGNALS. INPUT: SINEWAVE OR NARROW-BAND "OPTICAL" (SINGLE-TUNED) NOISY "SIGNAL", IN NARROW-BAND "OPTICAL" NOISE.

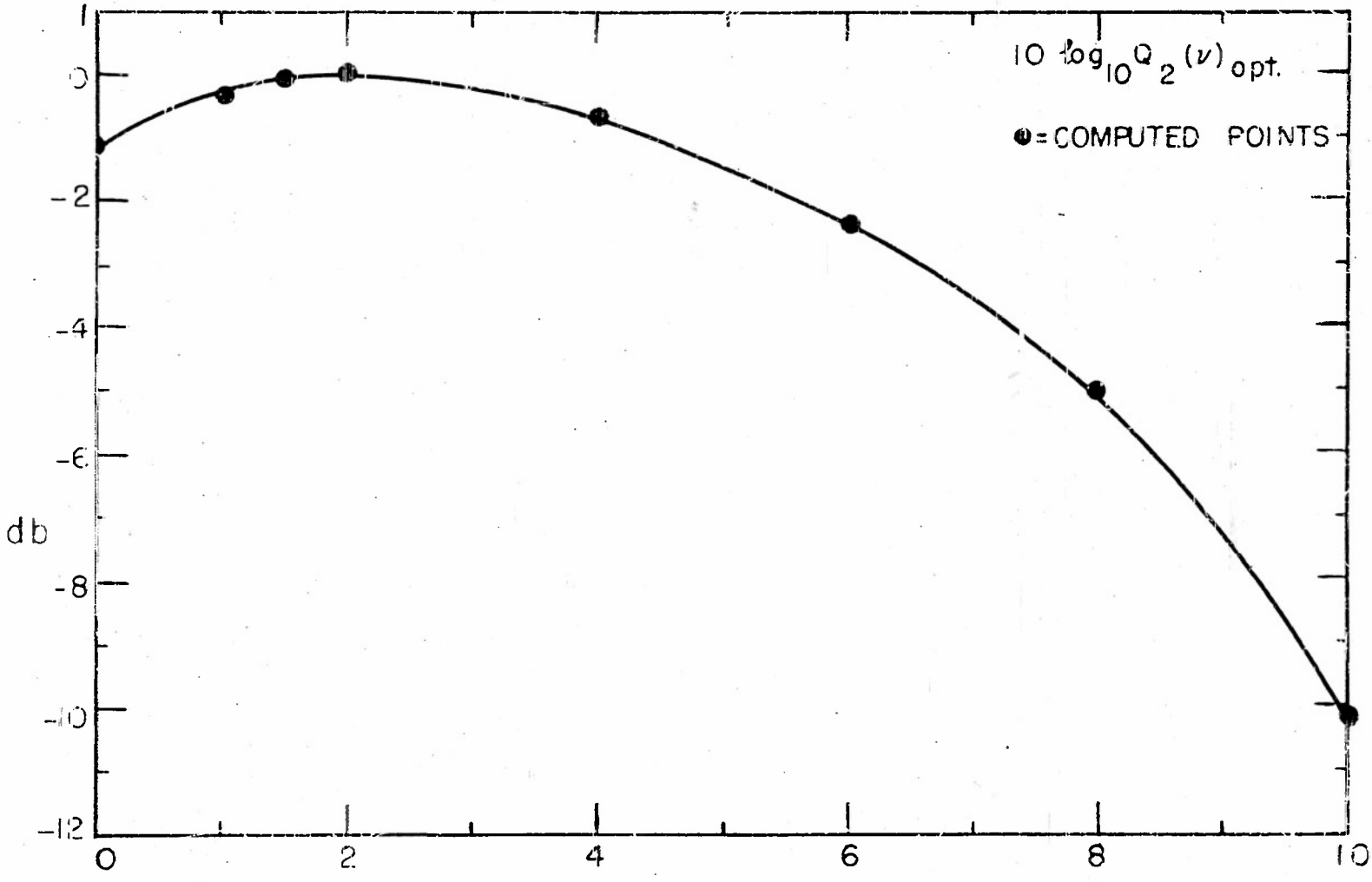

FIG. 13 $10 \log_{10} Q_2(\nu)_{opt.}$; P/p^2 FOR WEAK INPUT: SINEWAVE IN BROAD-BAND "OPTICAL" NOISE.

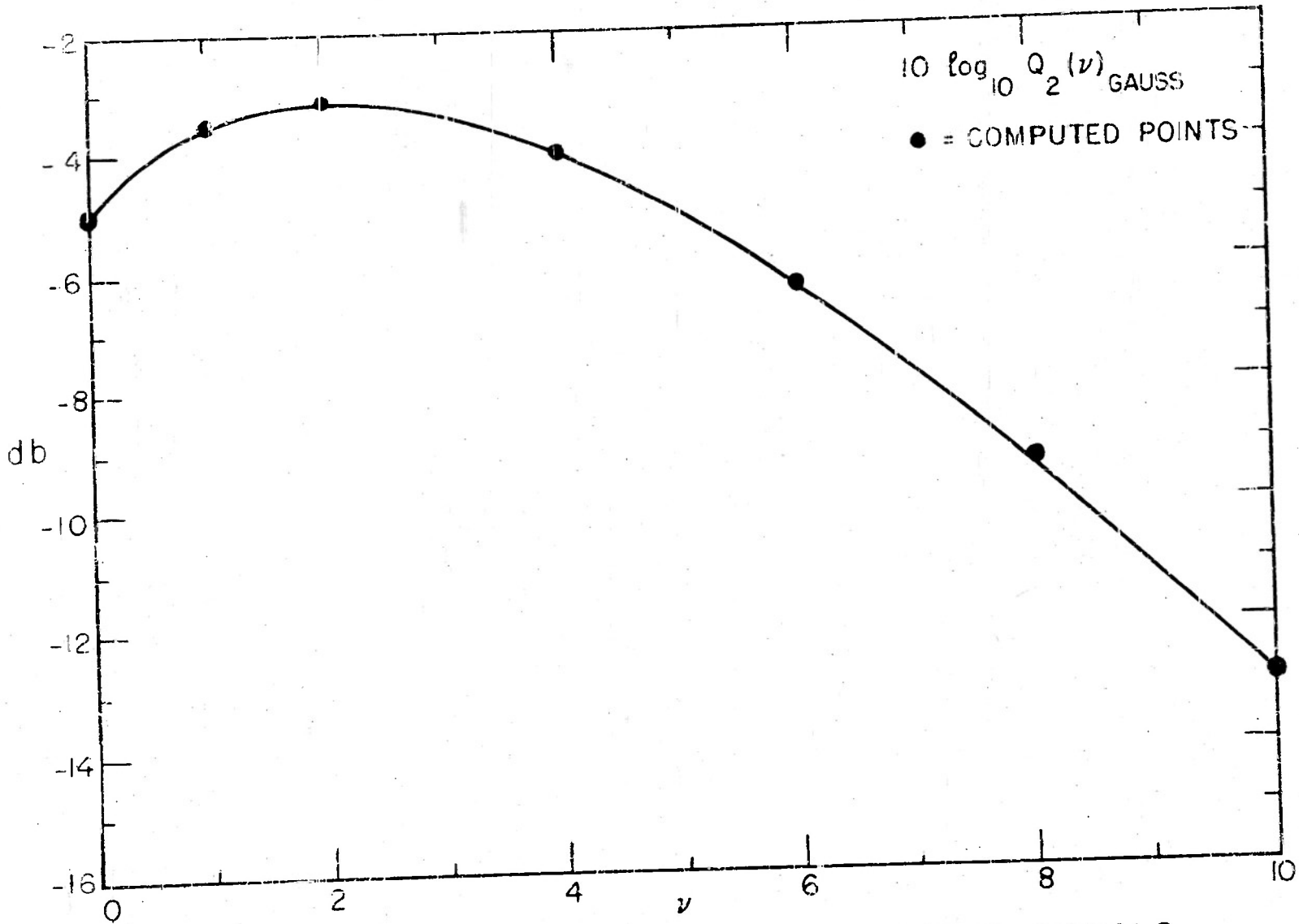

FIG. 14 $10 \log_{10} Q_2(\nu)_{GAUSS}$; P/p^2 FOR WEAK INPUT SIGNALS.
INPUT: SINEWAVE IN BROAD-BAND "GAUSS" NOISE.

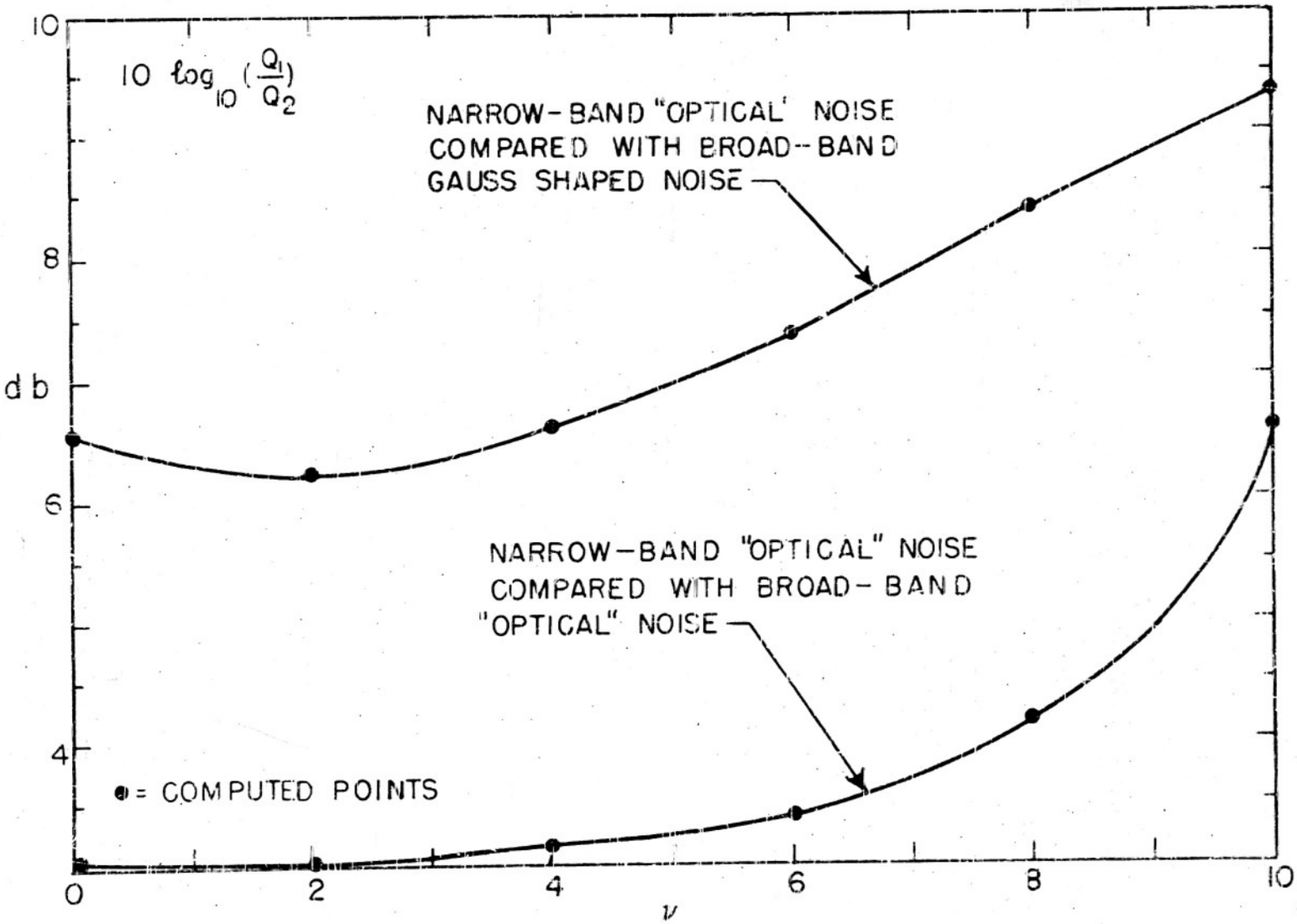

FIG. 16 INTRINSIC GAIN IN $P_{N.B.}$ OVER $P_{B.B.}$

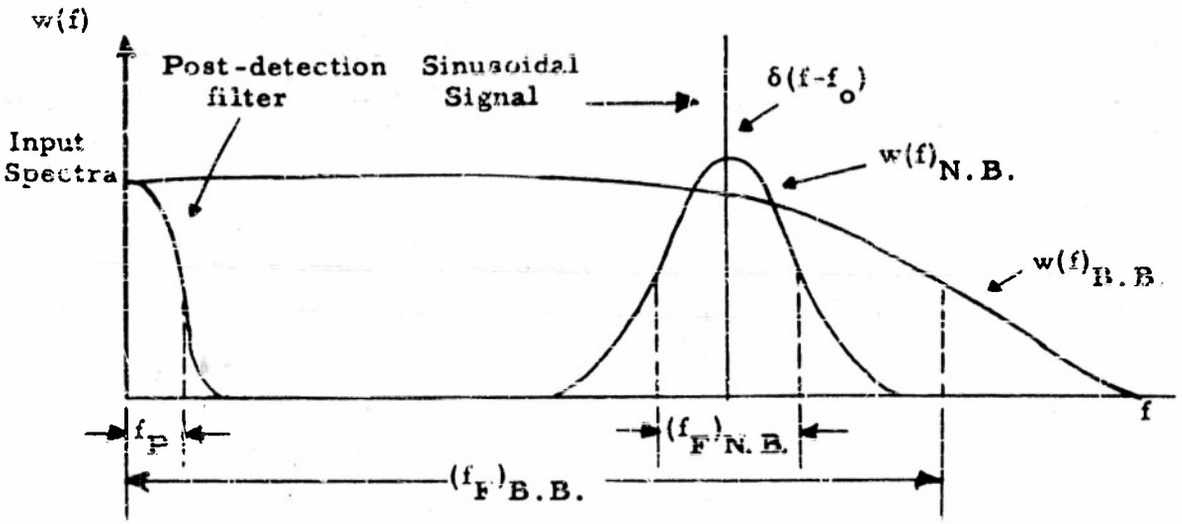

Fig. 15. Representation of weak signal detection schemes for a sine-wave in narrow-band noise as compared to broad-band noise.

general class of detectors. The types of narrow-band and broad band spectra chosen are described in (4.2) ac narrow-band "optical," to be compared to broad-band "optical," (4.4) and broad-band gaussian spectra (4.5). Figures 12-14 provide the data used in obtaining Fig. 1f

At the strong signal levels, significant differences in performance for the various types of input signal (e.g., sinusoidal or noise) appear in the output signal-to-noise ratio. In the case of a sinusoidal signal in narrow-band noise, or in broad-band noise, a simple dependence on the input ratio p is observed for $\nu > 1$: [cf. eqs. (8.12) and (10.26), (10.27)].

$$(\frac{2}{\pi})(\frac{\omega_P}{\omega_F})\, P_{N.B.} \simeq Q_3(\nu)p, \text{ case 1(a), or} \qquad (4.13)$$

$$(\frac{2}{\pi})(\frac{\omega_P}{\omega_F})\, P_{B.B.} \simeq Q_4(\nu)p; \text{ case 2(a).} \qquad (4.14)$$

(The behavior of $Q_3(\nu)$, $Q_4(\nu)$ is sketched in Fig. 17 in much the same manner as was done for small p.) However, there is a noticeable difference between what may and may not be plotted at the two extremes of input s/n. In the

threshold case ($p<1$), the curves for Q_1 and Q_2 are only approximate, since there is actually a slight dependence on p in the true expression for P, before approximation. However, this dependence on p is very slight (vanishing as $p\to 0$); and it does not change the general shape of the curve significantly, being easily accommodated for without changing our previous arguments. For large values of the input (s/n) ratio on the other hand, no representation of Q_3 and Q_4 for all (large) p is possible in the range around $\nu = 0$ (the case of extreme clipping). This follows from the fact that $Q_3(\nu)$ and $Q_4(\nu)$ vary as $1/\nu^2$. Thus, in this region ($0<\nu<1$) "separated" expressions of the types (4.13) and (4.14) cannot be properly written. Instead, a suitable modification of Q_3 and Q_4, depending on p, is needed. Note from Fig. 17 that Q_3 and Q_4 approach the limit-curve

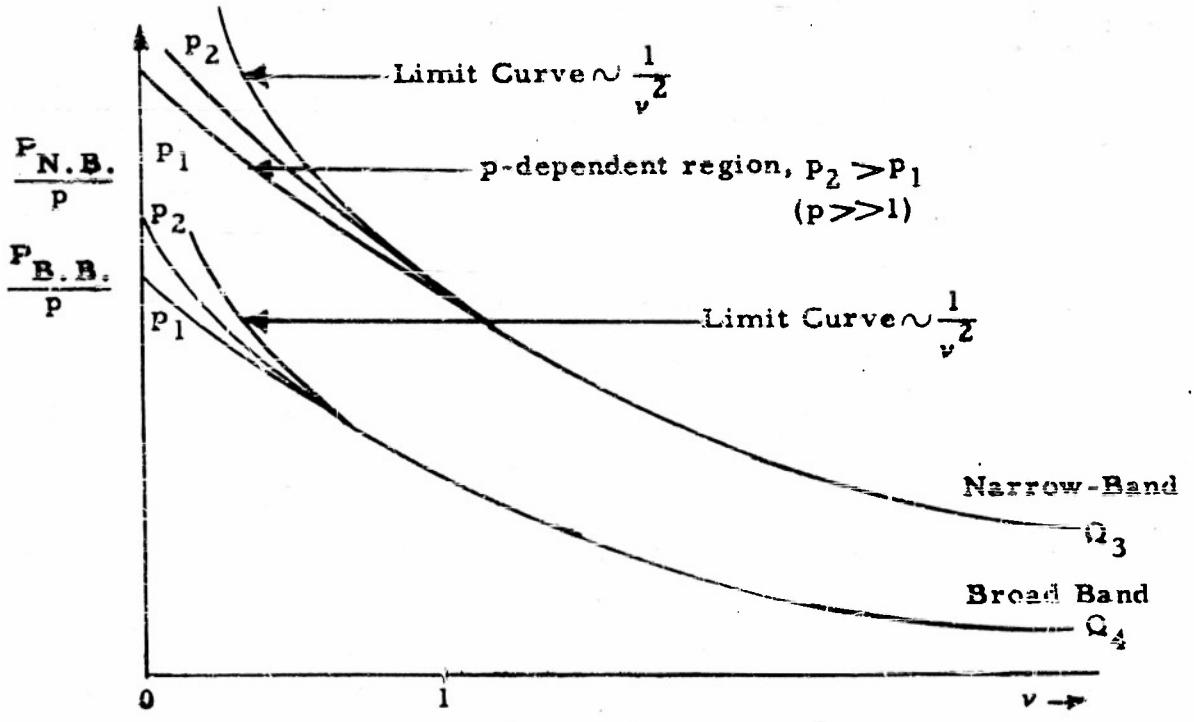

Fig. 17. Dependence of P on ν for large p, and a sinusoidal signal.

as p becomes larger. This means that the fluctuation noise vanishes much more rapidly than the d-c increment when ideal clipping ($\nu = 0$) is used. The limit-curves set an upper bound on P as p is made larger (for the

particular device in use).

The significant difference between noise and sinusoidal inputs is brought out by the fact that (for a narrow-band noise "signal" in a narrow-band noise background, where $p \gg 1$), the output power ratio P is virtually independent of p, viz.,

$$\left(\frac{2}{\pi}\frac{\omega_P}{\omega_F}\right)(P_{noise})_{N.B.} = Q_5(\nu) \ , \quad p \gg 1 \ , \text{ case 1(b)} \tag{4.15}$$

The quantity Q_5 exhibits the same type of behavior as Q_3 and Q_4 in the "clipping" ($\nu < 1$) and "amplifying" ($\nu > 1$) regions. In the latter, P is independent of p because the input "signal" itself is a noise wave, providing most of the fluctuation noise itself (strong "signal" case), even as it also supplies most of the d-c increment. Thus, both the output signal and fluctuating background increase at the same rate for a given detector law ($\nu > 1$).

For very large input signal-to-noise ratios, the ideal clipper is characterized by the greatest output signal-to-noise ratio. Over all values of input (s/n), the output signal-to-noise ratio for the ideal clipper is [eq. (9.9)],

$$\left(\frac{2}{\pi}\frac{\omega_P}{\omega_F}\right)(P_{noise})_{N.B.} = 1.672\,[\ln(1+p)]^2$$

$$\simeq 1.672\,p^2 \ , \quad p \ll 1 \ . \tag{4.16}$$

It is to be noted that the characteristic p^2 dependence for weak signals is present here (4.16). No such simple relation as (4.16) exists for a sinusoidal signal for all values of p. However, for strong signals, we have

$$\left(\frac{2}{\pi}\frac{\omega_P}{\omega_F}\right)P = (\ln p + 0.577)^2\,p \ ; \text{ case 1(a)} \ , \quad p \gg 1 \tag{4.17}$$

$$\left(\frac{2}{\pi}\frac{\omega_P}{(\omega_F)_C}\right)P = \frac{1}{2}(\ln p + 0.577)^2\,p \ ; \text{ case 2(a)} \ , \ p \gg 1 \tag{4.18}$$

$$\left(\frac{2}{\pi}\frac{\omega_P}{(\omega_F)_C}\right)P = \frac{1}{1.77\sqrt{\pi}}(\ln p + 0.577)^2\,p \ ; \text{case 2(a)}, \ p \gg 1 \ . \tag{4.19}$$

We remark that, except for some general qualitative statements, no investigation of case 2(b) (a narrow-band noise "signal" in a background of broad-band noise) has been carried out. *

The previous discussion may be summarized in Fig. 18 opposite, the salient features of which have been remarked upon; the exact curves, Figs. 19-24 follow, with the analytical results appearing in the body of the report. (Part III, secs. 8, 9, 10).

The effect upon P (the output signal-to-noise power ratio) of presenting a variety of inputs (cases 1(a) to 2(a)) to the νth-law devices ($\nu = 0, 1, 2$) at extremes of input signal-to-noise ratios, are summarized in Table I. The quantity referred to in each case is specifically $(\frac{2}{\pi} \frac{\omega_P}{\omega_F}) P$. The quantity tabulated in rows 7 and 8 respectively are $(\frac{2}{\pi} \frac{\omega P}{(\omega_F)_o}) \underline{P}$ and $(\frac{2}{\pi} \frac{\omega P}{(\omega F)_G}) \underline{P}$. If the input noise powers from these two filters, optical and Gauss, are required to be the same for a given signal, then eq. (4.6) must be applied,

$$(\omega_F)_G = \sqrt{\pi}\, (\omega_F)_o . \tag{4.20}$$

Quantities in row 8 are therefore multiplied by $\sqrt{\pi}$ if we compare $(\frac{2}{\pi} \frac{\omega P}{(\omega_F)_o}) P$ in row 7 with the same quantity in row 8; e.g., a signal of a given power must be accompanied by a noise of equal power from each filter. Moreover, comparison of identical quantities at the output are required to express $(\frac{\omega P}{(\omega_F)_o}) P$ for both types of spectral input.

---

* In this case, P depends not only on ν, but on a ratio of bandwidth of "signal" and noise.

Table 1

Case	Description, Input	p	$\nu = 0$	$\nu = 1$	$\nu = 2$	Row
1(a)	Sinusoidal signal in narrow-band noise	$p \ll 1$	$1.672\ p^2$	$1.928\ p^2$	$2.00\ p^2$	1
		$p \gg 1$	$\frac{(\ln p + 0.557)^2 p}{2}$	$2.00\ p$	$\frac{p}{2}$	2
1(b)	Narrow-band noise "signal" in narrow-band noise	$p \ll 1$	$1.672\ p^2$	$1.982\ p^2$	$2.00\ p^2$	3
		$p \gg 1$	$1.672\ p^2$	7.70	2.00	4
2(a)	Sinusoidal signal in broad-band noise (optical spectrum)	$p \ll 1$	$0.77\ p^2$	$0.95\ p^2$	$1.00\ p^2$	5
		$p \gg 1$	$\frac{(\ln p + 0.577)^2 p}{4}$	$1\ p$	$\frac{p}{4}$	6
2(b)	Sinusoidal signal in broad-band noise (Gauss spectrum)	$p \ll 1$	$0.32\ p^2$	$0.446\ p^2$	$0.48\ p^2$	7
		$p \gg 1$	$\frac{(\ln p + 0.577)^2 p}{3.54\sqrt{\pi}}$	$\frac{4p}{3.54\sqrt{\pi}}$	$\frac{p}{3.54\sqrt{\pi}}$	8

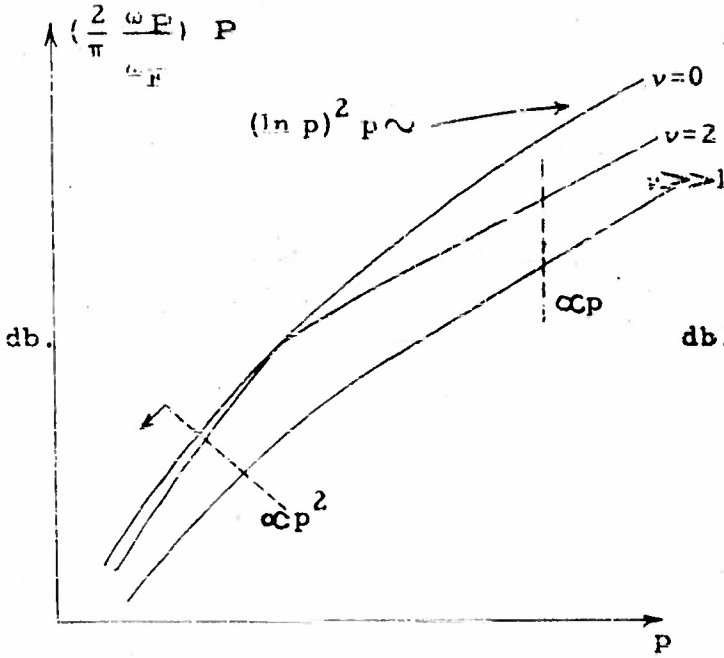

Fig. 18(a) Case 1(a), sine wave in narrow-band noise (cf. Fig 19)

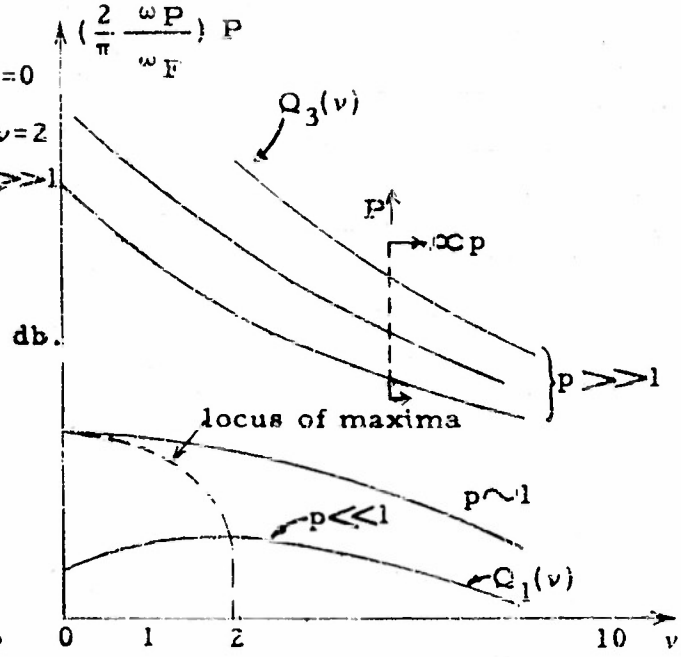

Fig. 18(b) Case 1(a), sine wave in narrow band noise (cf. Fig. 20)

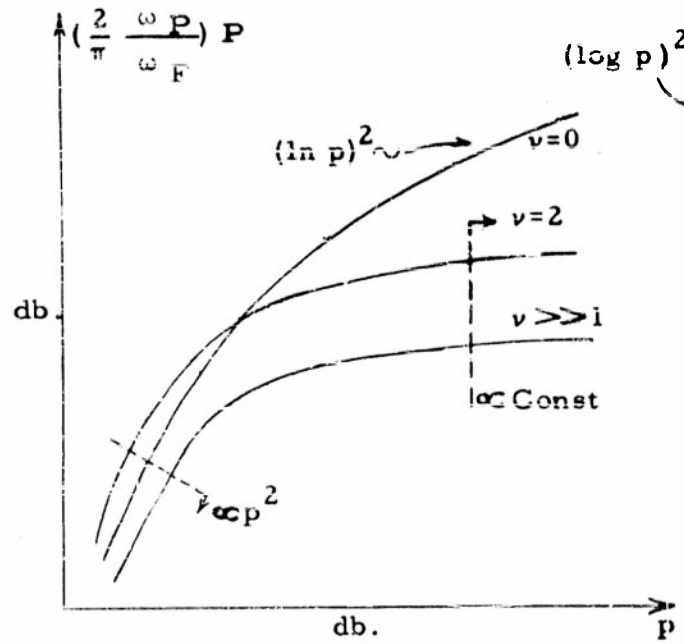

Fig. 18(c) Case 1(b), narrow-band noise "signal" in narrow-band noise background (cf. Fig. 21)

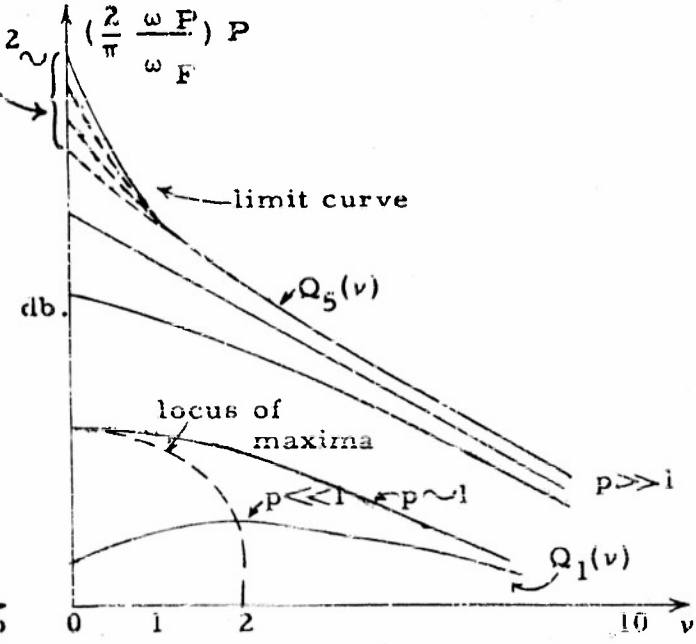

Fig. 18(d) Case 1(b), narrow-band noise "signal" in narrow-band noise background (cf. Fig. 22)

Fig. 18. Output signal-to-noise power ratio, P, for the cases considered in the discussion, illustrating variations and features discussed.

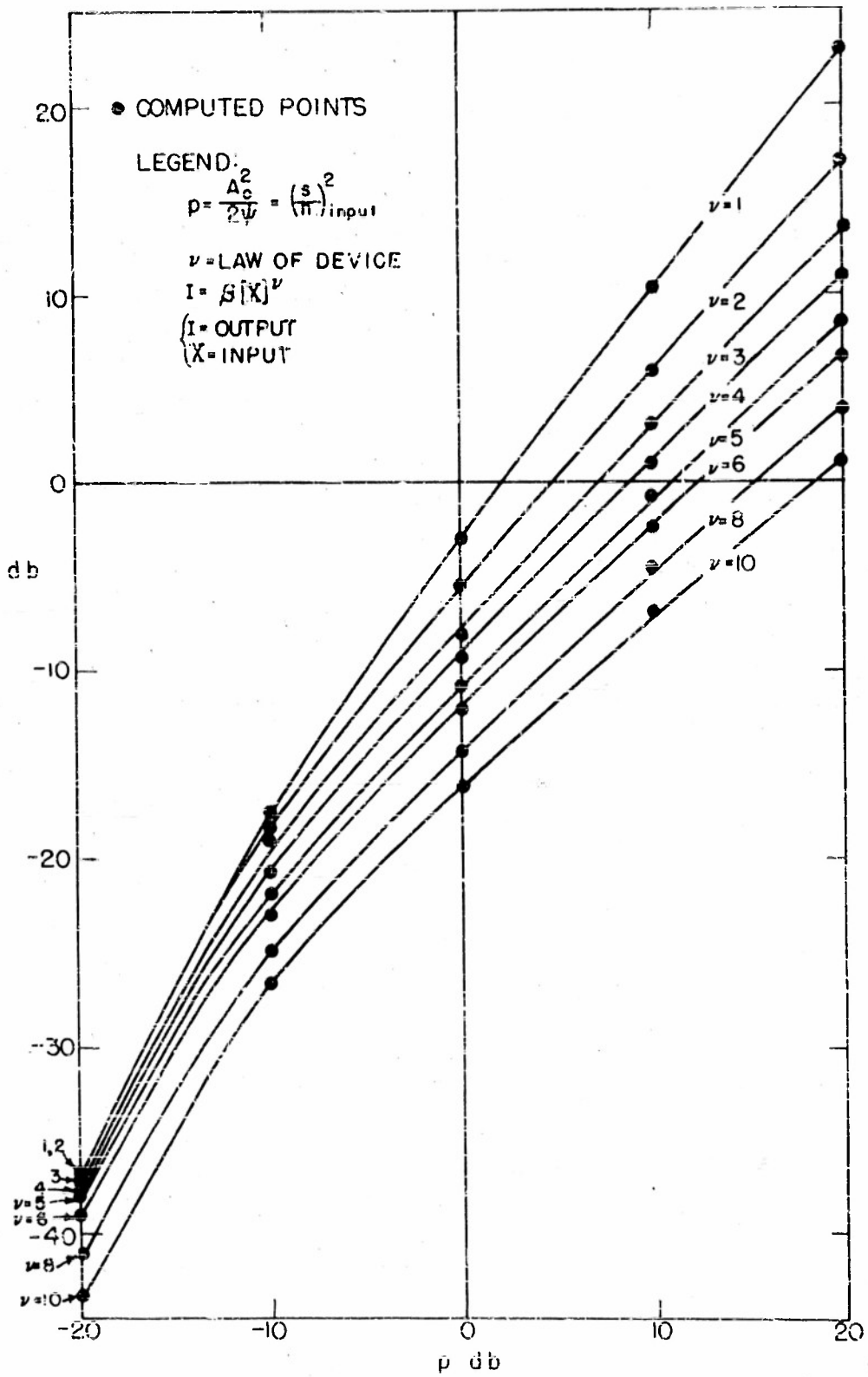

FIG. 19 OUTPUT (S/N) AS A FUNCTION OF INPUT (s/n) FOR VARIOUS ν^{th} LAW DEVICES. INPUT: SINUSOIDAL SIGNAL AND NARROW-BAND NOISE.

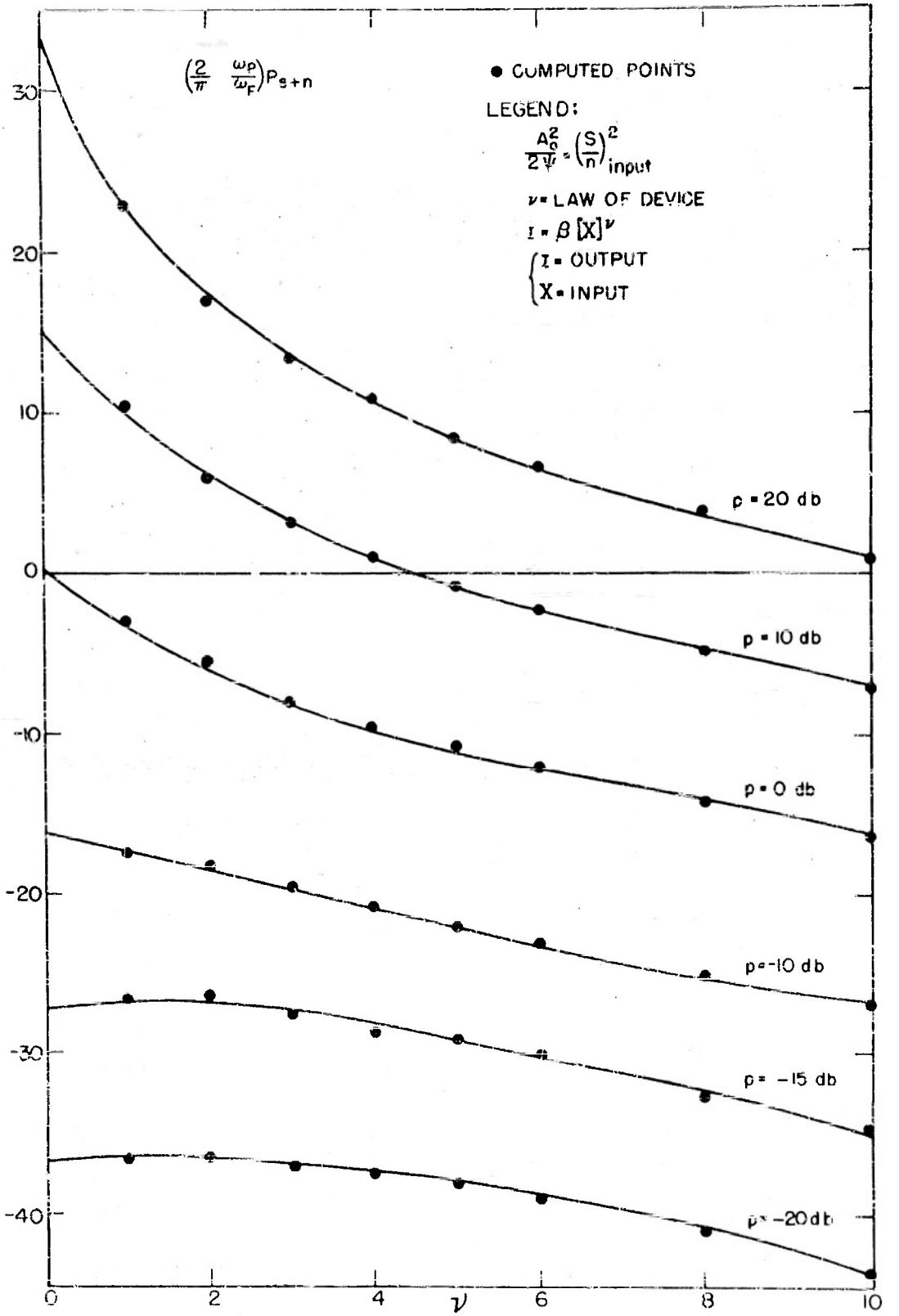

FIG. 20 OUTPUT (S/N) FOR VARIOUS INPUT (s/n) LEVELS, AS A FUNCTION OF THE ν^{th} LAW DEVICE. INPUT: SINUSOIDAL SIGNAL AND NARROW-BAND NOISE.

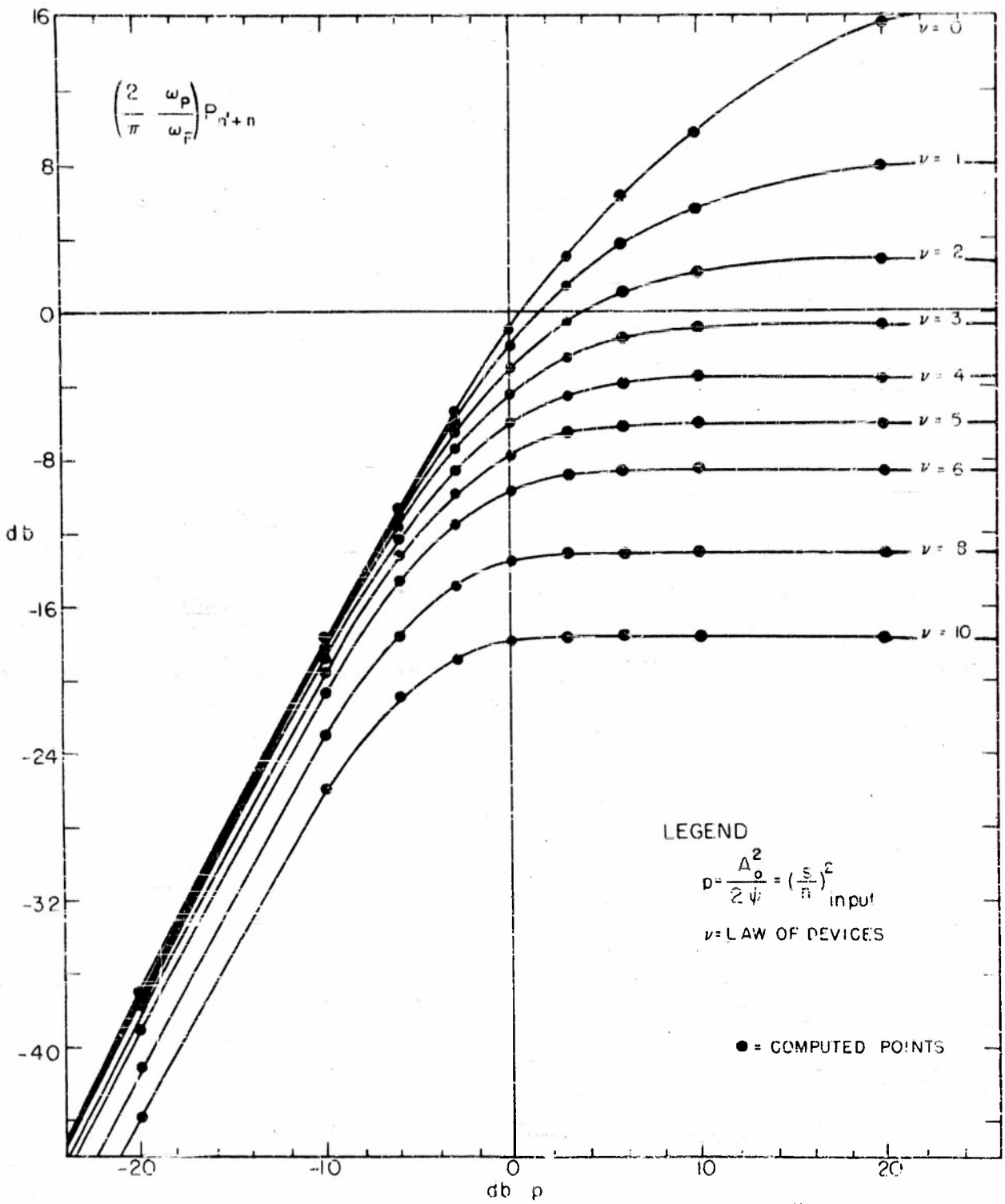

FIG. 21 OUTPUT (S/N) AS A FUNCTION OF INPUT (s/n) FOR VARIOUS ν^{th} LAW DEVICES. INPUT: NARROW-BAND "NOISE"-SIGNAL IN NARROW-BAND NOISE.

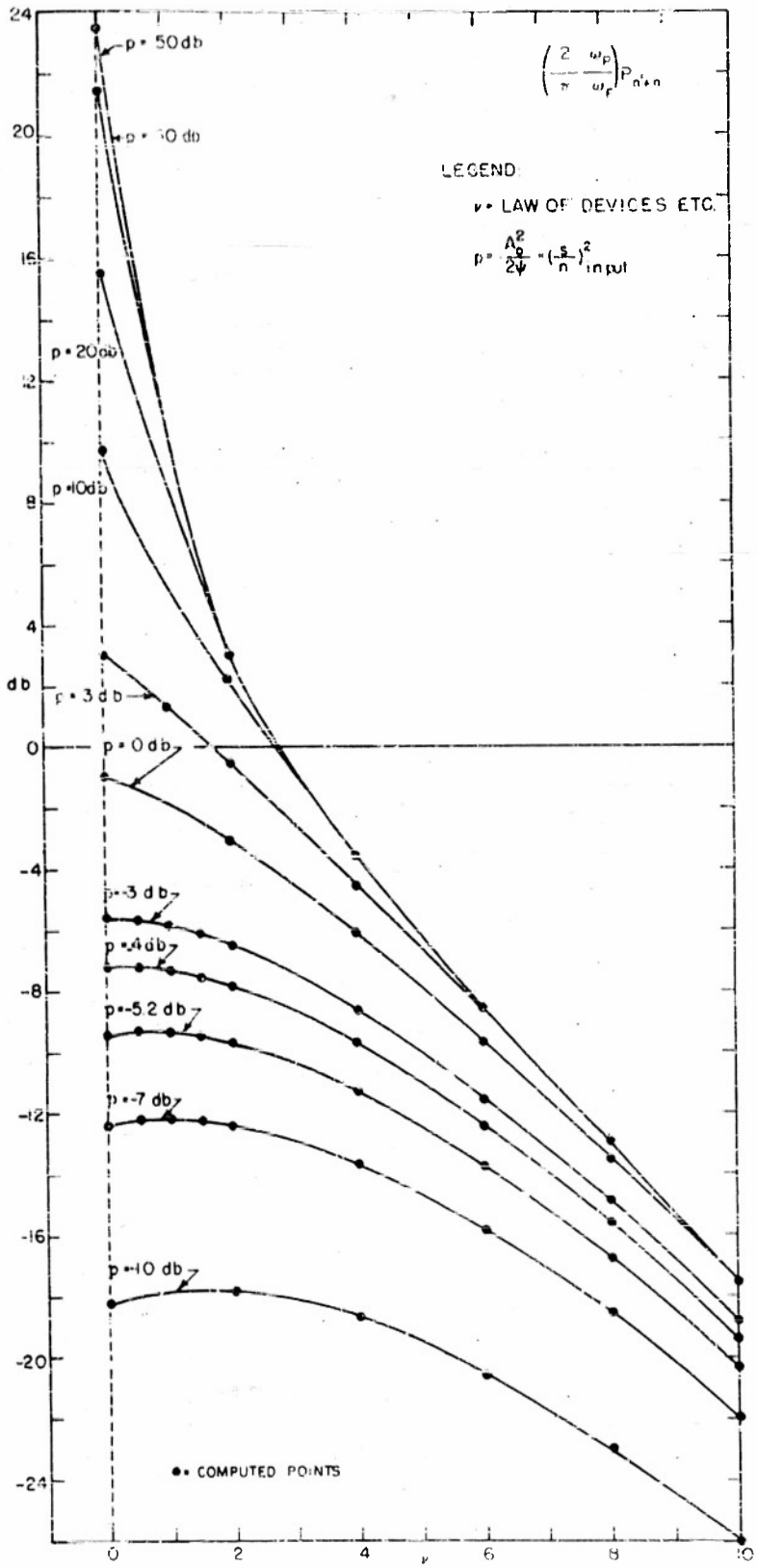

FIG. 22 OUTPUT (S/N) FOR VARIOUS INPUT (s/n), AS A FUNCTION OF LAW OF RECTIFIER. INPUT: NARROW-BAND 'NOISE'+ SIGNAL IN NARROW-BAND NOISE.

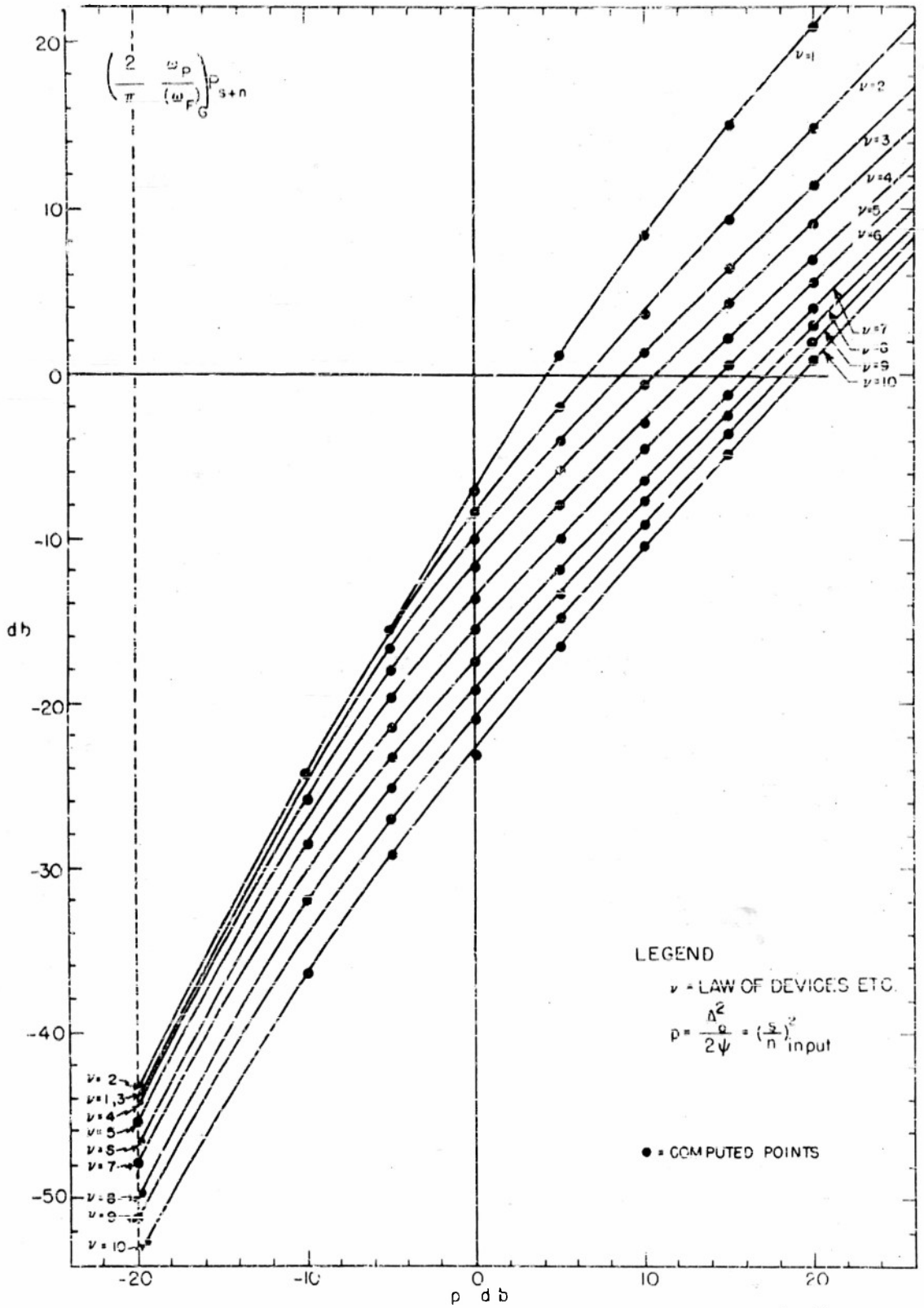

FIG. 23 OUTPUT (S/N) AS A FUNCTION OF INPUT (s/n) FOR VARIOUS ν^{th} LAW DEVICES, INPUT: SINUSOIDAL SIGNAL IN BROAD-BAND NOISE WITH GAUSS SPECTRUM.

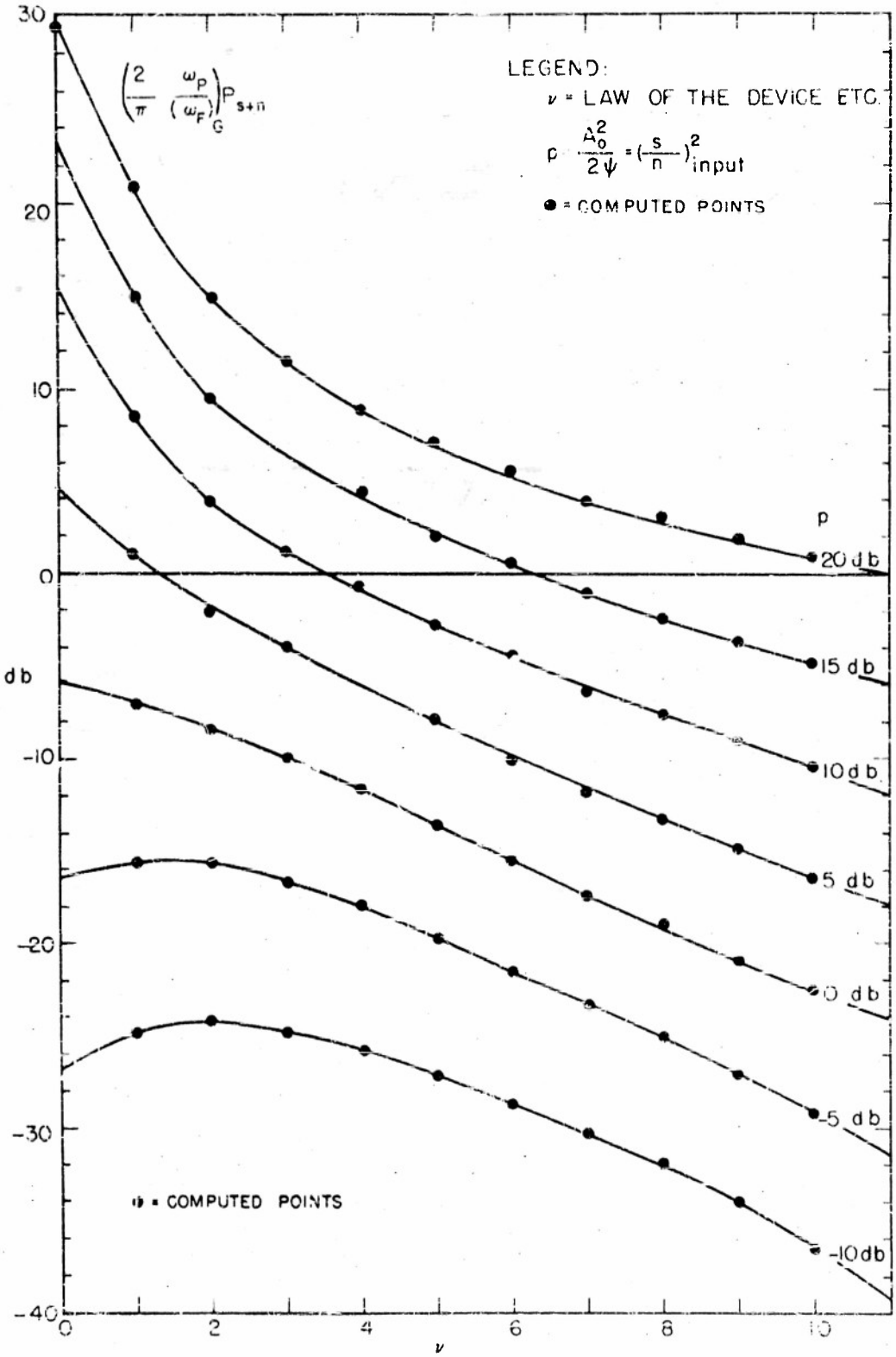

FIG 2.4 OUTPUT (S/N) FOR VARIOUS INPUT (s/n) LEVELS, FOR A ν^{th} LAW DEVICE. INPUT: SINUSOIDAL SIGNAL IN BROAD-BAND NOISE, GAUSS SPECTRUM.

II.

Analytical Section

5. Assumptions

The following problems are presented and solved: to find the correlation function for the output of a νth-power-law rectifier when the input is

(i) noise alone

(ii) noise and an uncorrelated signal as described in Part I, cf. cases 1(a) - 2(b).

The conditions which the nonlinear element is to obey are

(1) the device is assumed to be frequency-independent. This is a realistic assumption for the following reasons. When the distributed reactance of the device has a negligible effect on a voltage in the frequency region under consideration, our assumption is valid ab initio. When such is not the case, the distributed reactance may be considered as belonging to the circuits associated with the device, as a first approximation. Frequency-dependence attributable to the associated circuits may be introduced by separate consideration of the effect of all reactive networks upon the spectrum, before or after the device.

(2) the value of ν is unrestricted and positive; i.e., $\nu \geq 0$, (cf. sec. 4, ref. 5.)

The conditions which the noise and signal at the input are assumed to obey are:

(1) the noise is stationary; i.e., the ensemble of possible noise waves remains invariant under an arbitrary linear time transformation.

(2) the noise belongs to a gaussian random process.

(3) the signal is stationary.

The results of this investigation are applicable to the calculation of (1) the output signal-to-noise ratio as a function of the input signal noise ratio, (as previously outlined). (2) the rms fluctuation at the output of an optimum linear-averaging element following the νth-law device; (3) comparison between full and half-wave detection in the above two instances.

6. The Output Correlation Function

We now review briefly the problem of obtaining the correlation function of the output for a stationary wave that has been passed through a general nonlinear device (cf. sec. 5.) If the input voltage is V, and the output current (or voltage) is I, then I and V are related by some function,

$$I = g(V) \quad . \tag{6.1}$$

Then, if $V(t_1)$ is some function of time, and $I(t_1)$ is a corresponding function of time, the output correlation function is

$$R(t) = \left\langle I(t_1)\, I(t_2) \right\rangle_{t_i} \tag{6.2}$$

The ergodic theorem implies that (6.2) can be replaced by*

$$R(t) = \left\langle g(X_1)\, g(X_2) \right\rangle_s = \iint g(X_1)\, g(X_2)\, W_2(X_1, X_2; t)\, dX_1\, dX_2 \tag{6.3}$$

in the usual way, where W_2 is the joint probability that the voltage V lies in the range X_1, $X_1 + dX_1$ at time t_1 and in the range X_2, $X_2 + dX_2$ at a time, t_2, which is t later than t_1. For the statistical average, $\left\langle \right\rangle_s$, X_1 refers to V(t) at some arbitrary time t_1, and X_2 to V at a later time t_2; $(t_2 - t_1 = t)$. The method is now applied to the problem of noise alone. We consider first

A. Broad-band Noise:

The nonlinear device is a full-wave rectifier whose dynamic characteristic is

$$g(X) = \beta \left| X \right|^{\nu} \qquad (\infty < X < \infty)\ ,\ \nu \geq 0 \quad . \tag{6.4}$$

The input is a gaussian noise, for which W_2, Eq. (6.3) is

$$W_2(X_1, X_2; t) = \frac{1}{2\pi\psi(1 - r^2)^{1/2}} \exp\left[-(X_1^2 + X_2^2 - 2rX_1X_2)/2\psi(1 - r^2) \right] \tag{6.5}$$

---

*If a process is ergodic, then the time average of a random variable is set equal (to within a set of functions of prob. measure zero) to the corresponding ensemble (statistical) average of the same random variable.

ψ = intensity of the noise = $\overline{V^2}$

r = r(t) = auto-correlation function for the input [r(0) = 1] .

To evaluate the integral (6.3) it is convenient to use a development of W_2 in terms of the Hermite functions (cf. Appendix A), viz.:

$$W_2(X_1,X_2;t) = \frac{1}{\psi} \sum_{m=0}^{\infty} \frac{(-1)^m}{m!} r(t)^m \left\{ \phi^{(m)}\left(\frac{X_1}{\psi^{1/2}}\right) \phi^{(m)}\left(\frac{X_2}{\psi^{1/2}}\right) \right\} \quad (6.6)$$

where $$\phi^{(m)}(v) = \frac{1}{\sqrt{2\pi}} \frac{d^m}{dv^m} e^{-\frac{v^2}{2}} = (-1)^m H_m(v) \frac{e^{-\frac{v^2}{2}}}{\sqrt{2\pi}} , \quad (6.7)$$

and $H_m(v)$ is a Hermite polynomial.[11] Substituting (6.6) into (6.3) gives finally

$$R(t) = 4 \sum_{m=0}^{\infty} \frac{[\psi r(t)]^m}{m!} h_{o,m}^2 , \quad (6.8)$$

where the amplitude functions $h_{o,m}$ are

$$h_{o,m} = \beta \left\{ \frac{1}{4\psi^{m+1}} \right\}^{1/2} \int_{-\infty}^{\infty} |x|^{\nu} \phi^{(m)}\left(\frac{x}{\sqrt{\psi}}\right) dx. \quad (6.9)$$

We remark, before continuing the analysis, that many of the results can be conveniently expressed in terms of hypergeometric functions, a number of which are already tabulated. Two types which appear frequently are

$$_2F_1(a,b;c;u) = \sum_{m=0}^{\infty} \frac{(a)_m (b)_m}{(c)_m} \frac{u^m}{m!}$$

where $(a)_m = a(a+1) \ldots (a+m-1) = \Gamma(a+m)/\Gamma(a)$

and $(a)_o = 1$

and $${}_1F_1(a,b;u) = \sum_{m=0}^{\infty} \frac{(a)_m}{(b)_m} \frac{u^m}{m!} .$$

Here, it is found that (6.8) can be written

$$R(t) = C_\nu \cdot {}_2F_1\left(-\frac{\nu}{2}, -\frac{\nu}{2}; \frac{1}{2}; r(t)^2\right) \qquad (6.10)$$

The constant C_ν appears frequently in our work. Its value is specifically

$$C_\nu = \frac{(2\psi)^\nu}{\pi} \cdot \left\{\beta\Gamma\left(\frac{\nu+1}{2}\right)\right\}^2 . \qquad (6.11)$$

B. Narrow-band Noise:

Narrow-band noise[5] possesses correlation function of the following form, if the noise spectrum is symmetrical about some central frequency, f_c:

$$r(t) = r_o(t) \cos \omega_c t . \qquad (6.12)$$

We find that

$$r(t)^{2m} = r_o(t)^{2m} \left[\frac{(2m)!}{2^{2m}}\right] \sum_{j=0}^{m} \epsilon_{2j} \frac{\cos 2j\omega_c t}{(m+j)!(m-j)!} ; \qquad (6.13)$$

Here ϵ_{2j} factor is one for $j = 0$, and two for all other indices. A useful identity here is

$$\frac{(2m)!}{2^{2m}} = m! \left(\frac{1}{2}\right)_m . \qquad (6.14)$$

When (6.13) is substituted into (6.10), and all contributions to the cos $2j\omega_c t$ terms are collected, we obtain for the correlation function after full-wave rectification of narrow-band noise

$$R(t) = \sum_{j=0}^{\infty} R_{2j} , \qquad (6.15a)$$

with

$$R_{2j} = [C_{\nu}{}' {}_{2j}] \left[\sum_{k=j}^{\infty} \frac{(-\frac{\nu}{2})_k^2 \, r_o(t)^{2k}}{(k-j)!\,(k+j)!} \right] \cos 2j\omega_c t \, . \qquad (6.15b)$$

Here R_{2j} is the contribution to the 2j'th spectral zone. The expression (6.15) is identical with the even-zone parts of the correlation function when a half-wave rectifier is employed. (Cf. ref. 5, page 481.)* After some manipulation, we obtain finally

$$R_{2j} = C_{\nu}{}' {}_{2j} (-\tfrac{\nu}{2})_j^2 \frac{r_o(t)^{2j}}{(2j)!} \cos 2j\omega_c t \; {}_2F_1(j-\tfrac{\nu}{2}; j-\tfrac{\nu}{2}; 2j+1; r_o(t)^2)$$

$$j = 0, 1, 2 \ldots \, . \qquad (6.16)$$

Since $(C_{\nu})_{\text{full-wave}} = 4\,(C_{\nu})_{\text{half-wave}}$,

the only difference for the even-zones outputs in the two types of rectification is that

$$[R(t)_{2j}]_{\text{full-wave}} = 4\,[R(t)_{2j}]_{\text{half-wave}} \, . \qquad (6.17)$$

For the low-frequency continuum, j = 0. the correlation function for a narrow-band noise output alone is simply

$$R(t)_o = C_{\nu} \cdot {}_2F_1(-\tfrac{\nu}{2}, -\tfrac{\nu}{2}; 1; r_o(t)^2) \, . \qquad (6.18)$$

Cf. Eq. (6.11), ref. (5).

7. Characteristic-Function Method

A. Output Correlation Function; Transforms

A technically more convenient approach is the so-called "characteristic-function method," which may be applied to both classes (1) and (2) of input, discussed in section 2. Consider first the general half-wave device,

- - - - - - -

*Even zones appear in the random noise case for the same reason as they do in the simple sinusoidal input case; a Fourier analysis of the output has for its fundamental frequency twice the fundamental of the input.

in which g(X) exists only for positive X, and

$$g(X) = 0 \quad , \quad X < 0 \; . \tag{7.1}$$

The transformed characteristic is then defined as:

$$f(i\xi) = \int_0^\infty g(X)\, e^{-(i\xi)X}\, dX \; , \quad \mathrm{Im}(\xi) < 0 \; . \tag{7.2}$$

Assume that g(X) does not diverge* faster than $e^{\gamma X}$, where γ is some positive constant. Equation (7.2) is simply a Laplace transform in the $z = i\xi$-plane. Thus, the following transform representation of g(X) is obtained:

$$g(X) = \frac{1}{2\pi} \int_{\underset{\sim}{C}} f(i\xi)\, e^{(i\xi)X}\, d\xi \; , \quad \mathrm{Im}(\xi) < 0 \; . \tag{7.3}$$

where $\underset{\sim}{C}$ is a contour along the real ξ-axis, with an indentation downward around zero to avoid a possible singularity, for γ equal to zero. If γ is not zero, then the contour would have to be shifted down along the imaginary ξ-axis an amount $-\gamma$. For the devices we consider, any contour arbitrarily close to the real ξ-axis is satisfactory.

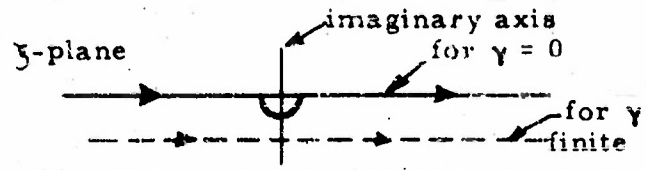

Fig. 25. The contour for evaluating g in the ξ-plane.

A canonical form for R is obtained:

$$R(t) = \frac{1}{4\pi^2} \int_{\underset{\sim}{C}_1} d\xi_1 \int_{\underset{\sim}{C}_2} d\xi_2\, f(i\xi_1)\, f(i\xi_2)\, F_2(\xi_1, \xi_2; t) \tag{7.4}$$

---

* This is physically quite reasonable, and perhaps even too strong a condition, since most electronic devices saturate at some input level, X_o, and for $X > X_o$, g usually remains constant or goes to zero.

where $$F(\xi_1, \xi_2; t) = \int_{-\infty}^{\infty} \int_{-\infty}^{\infty} W_2(X_1, X_2; t)\, e^{i(\xi_1 X_1 + \xi_2 X_2)}\, dX_1\, dX_2 \,. \tag{7.5}$$

Here, F_2 is the characteristic function of the probability distribution, W_2, i.e., its Fourier transform, which possesses convenient properties for our work, as will be seen.

The full-wave case now can be obtained by a generalization of the half-wave case. The most general type of full-wave response may be expressed as the sum of an even and an odd part:

$$g(X) = g_e(X) + g_o(X) \,,$$

with the properties

$$g_e(X) = g_e(-X) \,,$$

$$g_o(X) = -g_o(-X) \,.$$

Consider first the even part. This is a function which is symmetric about the g-axis. Treating the positive and negative halves of $g(X)$ as being half-wave devices, we may write:

$$g_e(X) = g'_e(X) + g''_e(X)$$

where

$$g'_e(X) = \frac{1}{2\pi} \int_C f_e(i\xi)\, e^{i\xi X}\, d\xi$$

$$g''_e(X) = \frac{1}{2\pi} \int_C f_e(i\xi)\, e^{i\xi(-X)}\, d\xi \,.$$

It is immediately obvious that $g''_e(X) = g'_e(-X)$. That is, the first contour integral vanishes for $X<0$, and takes on the values of $g_e(X)$ for $X>0$, while the second contour integral vanishes for $X>0$, and takes on the values of $g_e(-X)$ for $X<0$. Similar considerations applied to the odd part of $g(X)$ result in the relations:

$$g_o(X) = g'_o(X) - g''_o(X)$$

$$g'_o(X) = \frac{1}{2\pi} \int_C f_o(i\xi)\, e^{i\xi X}\, d\xi$$

$$g''_o(X) = \frac{1}{2\pi} \int_C f_o(i\xi)\, e^{i\xi(-X)}\, d\xi \quad .$$

Therefore, in general, we have

$$g(X) = \frac{1}{\pi} \int_C f_e(i\xi) \cos \xi X\, d\xi + \frac{i}{\pi} \int_C f_o(i\xi) \sin \xi X\, d\xi \quad . \qquad (7.6)$$

$g(X)$ we specialize in this report to $g_e(X)$, $(g_o = 0)$, so that g becomes

$$g(X) = \frac{1}{\pi} \int_C f(i\xi) \cos \xi X\, d\xi \quad . \qquad (7.7)$$

The output correlation-function after full-wave rectification thus is seen to be,

$$R(t) = \frac{1}{4\pi^2} \int_{C_1} d\xi_1 \int_{C_2} d\xi_2\, f(i\xi_1)\, f(i\xi_2)\, \Phi_2(\xi_1, \xi_2; t) \qquad (7.8)$$

where

$$\Phi_2(\xi_1, \xi_2; t) = \int\int_{-\infty}^{\infty} 2\left[\cos(\xi_1 X_1 + \xi_2 X_2) + \cos(\xi_1 X_1 - \xi_2 X_2)\right]$$

$$\cdot\, W_2(X_1, X_2; t)\, dX_1\, dX_2 \quad .$$

Recalling the definition of the characteristic function (7.5) we easily see that

$$\Phi_2(\xi_1, \xi_2; t) = F_2(\xi_1, \xi_2; t) + F_2(-\xi_1, -\xi_2; t) + F_2(-\xi_1, \xi_2; t) + F_2(\xi_1, -\xi_2; t). \qquad (7.9)$$

Here the first two terms are equal,* as are the last two, so that

$$\Phi_2(\xi_1, \xi_2; t) = 2[F_2(\xi_1, \xi_2; t) + F_2(-\xi_1, \xi_2; t)] . \qquad (7.10)$$

For example, for normal random noise we recall that

$$F_2(\xi_1, \xi_2; t) = \exp\left[-\frac{\psi}{2}(\xi_1^2 + \xi_2^2 + 2\xi_1\xi_2 r(t)\right] . \qquad (7.11)$$

If the input is a sinusoidal signal, we find that[5]

$$F_2(\xi_1, \xi_2; t) = \sum_{m=0}^{\infty} (-1)^m \epsilon_m J_m(A_o\xi_1) J_m(A_o\xi_2) \cos m\omega_o t , \qquad (7.12)$$

the amplitude of the signal being A_o, and f_o its frequency. In (7.12) we observe that

$$J_m(-u) = (-1)^m J_m(u) ,$$

so that (7.10) applies for a sinusoid, as well as noise. Accordingly, in the present cases we can write finally

$$R(t) = \frac{1}{2\pi^2} \int_{C_1} d\xi_1 \int_{C_2} d\xi_2 f(i\xi_1) f(i\xi_2) \left\{ F_2(\xi_1, \xi_2; t) + F_2(-\xi_1, \xi_2; t) \right\} . \qquad (7.13)$$

B. Broad-band Noise

Here we obtain from (7.11) for (7.13)

$$F_2(\xi_1, \xi_2; t) + F_2(-\xi_1, \xi_2; t) = 2 \exp\left[-\frac{\psi}{2}(\xi_1^2 + \xi_2^2)\right] \cosh\left[\psi\xi_1\xi_2 r(t)\right] . \qquad (7.14)$$

If the hyperbolic cosine is expanded in a power series, and the results substituted into (7.13) there results

$$R(t) = 4 \sum_{n=0}^{\infty} \frac{[\psi r(t)]^{2n}}{(2n)!} h_{o,2n}^2 , \qquad (7.15)$$

* For symmetrical distributions only.

And in particular

$$h_{o,2n} = \frac{1}{2\pi} \int_C f(i\xi)\, \xi^{2n} e^{-\frac{\psi}{2}\xi^2}\, d\xi . \qquad (7.16)$$

The relation (7.15) which follows from the characteristic-function method is seen to be formally identical with (6.8), with $m = 2n$. In the direct method of sec. 6 the terms for odd m are eliminated (cf. Appendix 1), so that the formal identity between the two methods is complete. The expression (7.16) for $h_{o,2n}$ occurs in R(t) when the half-wave νth-law detector is investigated.[5] The only difference between the full- and half-wave responses lies in the fact that the odd terms $h_{o,2n+1}$ are missing in the full-wave operation, and the full-wave expression for R(t) is multiplied by an additional factor 4. (The integrals $h_{o,2n}$ may be evaluated by the method shown in Appendix B.) The case of narrow-band noise input alone has been previously treated in sec. 6B.

C. Sinusoidal Signal and Broad-band Noise

It is well known that the characteristic function of the sum of independent variables is equal to the product of the characteristic functions of each of the variables.[12] Thus, if the input to a nonlinear device is a sum of two independent voltages (e.g., sinusoid and noise) we may write

$$F_2(\xi_1, \xi_2; t)_{s+n} = F_2(\xi_1, \xi_2; t)_s\, F_2(\xi_1, \xi_2; t)_n . \qquad (7.17)$$

where the subscripts s and n refer respectively to signal and noise. With the help of (7.11) and (7.12) R may be expressed as

$$R(t) = 2 \sum_{m,n=0}^{\infty} \epsilon_m [(-1)^{m+n} + 1] \frac{[\psi r(t)]^n}{n!} H_{mn}^2 \cos m\omega_o t , \qquad (7.18)$$

where H_{mn} is the amplitude function

$$H_{mn} = \frac{1}{2\pi} \int_C f(i\xi)\, \xi^n\, J_m(A_o\xi)\, e^{-\frac{\psi}{2}\xi^2}\, d\xi . \qquad (7.19)$$

Note for $m = 0$, and $A_o \to 0$ that H_{on} reduces to our previous integrals, $h_{o,n}$, so that

$$\lim_{A_o \to 0} H_{on} = h_{o,n} \qquad (7.20)$$

and

$$\lim_{A_o \to 0} H_{mn} = 0 \; ; \; m \neq 0 .$$

since $J_m(A_o\xi)$ vanishes as $A_o \to 0$. As expected for vanishing signal (7.18) reduces to precisely the expression (7.15) for noise alone. The first half of the sum (7.18), containing the factor $(-1)^{m+n}$, is exactly the half-wave expression for a sinusoidal signal in noise. The second half of the sum, (that containing the term 1) removes terms for which $(m + n) = 2\ell + 1$. Then R may be simply written:

$$R(t) = 4 \sum_{\substack{m+n=2\ell \\ \ell=0,1,\ldots}}^{\infty} \left[\frac{\epsilon_m H_{mn}^2}{n!}\right] [\psi r(t)]^n \cos m\omega_o t . \qquad (7.21)$$

D. Remarks on (s X n) Noise Terms

Before examining the complete expression which arises from (7.21) for the νth-law device, we present a short discussion of (7.18). First, examination of H_{mn} reveals that the integral (7.19) represents a (signal-device-noise) interaction term, in matrix form: $(m|f|n)$, corresponding to the signal statistics $[J_m(A_o\xi)]$, the device $f(i\xi)$, and the noise statistics $\xi^n \exp(-\frac{\psi}{2}\xi^2)$; m and n referring formally to statistical "states" of the signal and noise. Since H_{mn} depends on A_o and ψ, as the input signal-to-noise power ratio

$$p = \frac{A_o^2}{2\sigma^2} \qquad (7.22)$$

changes, so H_{mn} is sensitive to this variation. Each state inside H_{mn} is associated with a time-dependent term outside of the integral, specified by the same state number.

The d.c. term in (7.21) is represented by H_{oo}, since $(0\,|f|\,0)$ is the only term associated with a constant in the time-dependent terms. Thus, it is immediately seen that

$$(W_{d.c.})_{S+N} = 4H_{oo}^2 \qquad (7.23)$$

represents the d.c. intensity at the output, with signal and noise as input. Since $(W_{d.c.})_N = \lim_{s \to 0} (W_{d.c.})_{S+N}$, from (7.20), the d.c. intensity for noise alone is:

$$(W_{d.c.})_N = 4h_{o,o}^2. \qquad (7.24)$$

The d.c. voltage increment, or output signal, is then

$$S_{out} = 2[H_{oo} - h_{oo}] \quad . \qquad (7.25)$$

Note that the output signal increment is independent of the narrow- or broad-band structure of the noise. The only difference between P for the two cases 1(b) and 2(b) arises from the fluctuation-noise in the output. The low-frequency continuum at $f = 0$ is from Eq. (3.8)

$$W(0) = 4\int_0^\infty R'(t)\,dt, \qquad (7.26)$$

where R' is that part of the correlation function yielding $(s\chi n)$, $(n\chi n)$ terms only (exclusive of d.c.); (7.26) depends upon integrals of the form

$$T_{mn} = \int_0^\infty r(t)^n \cos m\omega_o t\,dt \quad . \qquad (7.27)$$

The value of (7.27) depends, of course, on whether or not the noise is broad- or narrow-band.

If N^2 represents the intensity of the noise fluctuations (low frequency output), from (7.21) we get

$$N^2 = 16 f_p \sum_{\substack{m+n=2\ell \\ \ell=1,2,3\ldots}}^{\infty} \epsilon_m \left[\frac{H_{mn}^2}{n!}\right] \psi^n T_{mn} \qquad (7.28)$$

and the output signal-to-noise (power) ratio is given by $P = (S/N)^2$:

$$\left(\frac{2}{\pi}\frac{\omega_F}{\omega_F}\right) P = \left[H_{oo} - h_{oo}\right]^2 / \omega_F \cdot \sum_{\substack{m+n=2\ell \\ \ell=1,2,3\ldots}}^{\infty} \epsilon_m \left[\frac{H_{mn}^2}{n!}\right] \psi^n \cdot T_{mn} \qquad (7.29)$$

Equation (7.29) indicates the manner in which P depends on the H_{mn} matrix and the T_{mn} "band-structure" factor. If $A_o \ll \sqrt{\psi}$, a case of interest to use here, Eq. (7.29) simplifies somewhat to

$$\left(\frac{2}{\pi}\frac{\omega_P}{\omega_F}\right) P \simeq h_o^2 / \omega_F \cdot \sum_{\substack{m+n=2\ell \\ \ell=1,2,3\ldots}}^{\infty} \frac{\epsilon_m h_{o}^{2}, n+m}{n!(m!)^2} \left(\frac{A_o}{2}\right)^{2(m-2)} \psi^n T_{mn} \qquad (7.30)$$

Equation (7.30) is convenient for calculating P, when the amplitude function $h_{o,2\ell}$ are known.

If a νth-law device is assumed, H_{mn} can be obtained (ref. 1, Eq. A. 3.14), so that the total R may be finally expressed as the following,

$$R(t) = C_\nu \Gamma\left(\frac{\nu}{2}+1\right)^2 \sum_{\substack{m+n=2\ell \\ \ell=0,1,\ldots}} \frac{\epsilon_m 2^n {}_1F_1^2 p^m}{(m!)^2 n! \Gamma\left(\frac{\nu}{2}+1-\ell\right)^2} \left[r(t)^n \cos m\omega_o t\right], \qquad (7.31)$$

Here ${}_1F_1 = {}_1F_1(\ell - \frac{\nu}{2}; m+1; -p)$ is the confluent-hypergeometric function [cf. (6.9) et seq.]. The separation of the important terms in (7.21) to obtain

$$W(0) = 4\int_0^\infty R'(t)\,dt$$

is carried out in Part III.

E. Sinusoidal Signal and Narrow-band Noise

For narrow-band noise, the above formalism is not convenient. Such a noise wave, having a symmetrical spectral distribution about a frequency f_c, possesses a normalized auto-correlation function which can be written

$$r(t) = r_o(t) \cos \omega_c t .$$

Let f_c be set equal to the signal frequency, f_o. Then the characteristic-function needed in the canonical form, (7.13) is:

$$\Phi_2(\xi_1, \xi_2; t)/2 = \sum_{\substack{m,q=0 \\ m+q=2\ell}} (-1)^{m+q} [\epsilon_m \epsilon_q] [J_m(A_o \xi_1) J_m(A_o \xi_2)]$$

$$\cdot [I_q(\psi r \xi_1 \xi_2)] [(\cos m\omega_o t)(\cos q\omega_o t)] . \qquad (7.32)$$

[In deriving (7.32) we have used the relation

$$e^{-z \cos \theta} = \sum_q (-1)^q I_q(z) \cos q\theta$$

where I_p is a modified Bessel-function.] When (7.32) is substituted into (7.13), and I_q is expanded in the series

$$I_q = I_{2\ell-m}(z) = \sum_{n=0}^{\infty} \frac{(z/2)^{2\ell-m+2n}}{(n!)(2\ell-m+n)!}$$

the following characteristic zonal structure appears:

$$R(t) = \sum_{\ell=0} R_{2\ell}(t) ,$$

with

$$R_{2\ell}(t) = 4\cos 2\ell\omega_o t \sum_{m,n=0}^{\infty} \frac{\epsilon_m [H_{m,|m-2\ell|+2n}]^2}{n!\,(n+|m-2\ell|)!} \left[\frac{\psi}{2} r_o(t)\right]^{2n+|m-2\ell|} \tag{7.33}$$

where $H_{m,2n+|m-2\ell|}$ has its previous significance.[5] The low-frequency zone, $\ell = 0$, is of greatest interest here; we find that

$$R(t)_o = 4 \sum_{m,n=0}^{\infty} \epsilon_m \frac{(H_{m,m+n})^2}{n!\,(m+n)!} \left[\frac{\psi}{2} r_o(t)\right]^{2n+m}. \tag{7.34}$$

For the νth-law device, $H_{m,2n+m}$ has been evaluated,[5] so that we can write explicitly

$$R(t)_o = C_\nu \sum_{m,n=0}^{\infty} \frac{\epsilon_m \left(-\frac{\nu}{2}\right)_{m+n}^2 \; {}_1F_1\left(m+n-\frac{\nu}{2};\, m+1;\, -p\right)^2}{(m!)^2\, n!\, (m+n)!}\, p^m\, r_o(t)^{2n+m}. \tag{7.35}$$

F Two Uncorrelated Broad-band Noise Waves

If the "signal" noise presented to the nonlinear device be indicated n' and the background noise is denoted by n, then for an input which is the sum of these two statistically independent noise waves, we have directly

$$F_2(\xi_1, \xi_2; t)_{n'+n} = F_2(\xi_1, \xi_2; t)_{n'}\, F_2(\xi_1, \xi_2; t)_n. \tag{7.36}$$

For gaussian noise this becomes

$$F_2(\xi_1, \xi_2; t)_{n'+n} = \exp\left[-\frac{\psi_T}{2}(\xi_1^2 + \xi_2^2)\right] \exp -\left[\psi r(t) + \psi' r'(t)\right] \xi_1 \xi_2 \tag{7.37}$$

where $$\psi_T = \psi + \psi' = \psi(1+p)$$

and the input (power) signal-to-noise ratio is

$$p = \frac{\psi'}{\psi}. \tag{7.38}$$

The expression ψ_T may replace ψ everywhere in the expression for

noise alone. We have, therefore,

$$R(t) = 4 \sum_{n=0}^{\infty} [\psi r(t) + \psi' r'(t)]^{2n} \frac{h_{o,2n}^{2}}{(2n)!} , \qquad (7.39)$$

where $h_{o,2n}$ now contains the factor ψ_T. For case 1(b) where both signal and noise have the same spectral shape, e.g., $r(t) = r'(t)$, we get at once

$$R(t) = 4 \sum_{n=0}^{\infty} \frac{[\psi_T r(t)]^{2n}}{(2n)!} (h_{o,2n})^{2} , \qquad (7.40)$$

which, as expected, is precisely the expression obtained for noise alone through $g(V)$, [except, of course, that ψ is ψ_T]. Then we can write also

$$R(t) = C_{\nu,p} \; {}_2F_1 \left(-\frac{\nu}{2}, -\frac{\nu}{2}; \frac{1}{2}; r(t)^2\right) \qquad (7.41a)$$

where

$$C_{\nu,p} = C_{\nu} (1+p)^{\nu} . \qquad (7.41b)$$

Where the spectra of this input noise wave have shapes [case 2(b)], then

$$R(t) = C_{\nu,p} \; {}_2F_1 \left(-\frac{\nu}{2}, -\frac{\nu}{2}; \frac{1}{2}; \left[\frac{r(t) + p r'(t)}{(1+p)}\right]^2\right), \qquad (7.42)$$

which, computationally, is rather an involved expression.

G. Two Uncorrelated Narrow-band Noise Waves

Here $R(t)$ is identical with the correlation function for noise alone, except that C_{ν} is replaced by $C_{\nu,p}$, as we have shown above. The zonal structure for two, narrow-band noise voltages after rectification, one of which is the "signal", the other of which is the "noise" (and both of which possess identical spectra), appears in the same way, except for the p-dependent multiplier $(C_{\nu,p})$. Therefore, for the low-frequency zone, we get

$$R(t)_o = C_{\nu,p} \; {}_2F_1 \left(-\frac{\nu}{2}, -\frac{\nu}{2} - 1; r_o(t)^2\right) . \qquad (7.43)$$

When the noise spectra are different, though still centered about the same spectral frequency f_o, we get, corresponding to (7.42),

$$R(t)_o = C_{\nu,p}\, {}_2F_1\left(-\frac{\nu}{2}, -\frac{\nu}{2}; 1; \left[\frac{r_o(t) + p\, r_o'(t)}{(1+p)}\right]^2\right) . \qquad (7.44)$$

III.

The Output Signal-to-Noise Ratio

8. Sinusoidal Signal in Narrow-band Noise

Using expression (7.35) for the low-frequency correlation function R(t) we find that the d-c terms constituting the signal are

$$(W_{d.c.})_{S+N} = C_\nu\, {}_1F_1\left(-\frac{\nu}{2}; 1; -p\right)^2 , \qquad (8.1)$$

$$(W_{d.c.})_N = C_\nu . \qquad (8.2)$$

Therefore, the d-c signal increment S is

$$S = \sqrt{C_\nu}\left[{}_1F_1\left(-\frac{\nu}{2}; 1; -p\right) - 1\right] . \qquad (8.3)$$

The fluctuation noise power, N^2, on the other hand, is given by

$$N^2 = 4C_\nu f_p \cdot \sum_{\substack{m,n \\ m+n\neq 0}} \frac{\epsilon_m \left(-\frac{\nu}{2}\right)^2 {}_1F_1\left(m+n-\frac{\nu}{2}; m+1; -p\right)^2}{n!\,(m+n)\,!\,(m!)^2} \cdot \int_c^\infty r_o(t)^{2n+m}\, dt \qquad (8.4)$$

and the d-c term, m,n=0 is excluded. If the pre-detection filter is a simple narrow-band RLC-tuned circuit, as shown in Fig. 26, then the correlation function of the input noise is given by

$$r(t) = r_o(t) \cos \omega_o t$$

with

$$\omega_o = \frac{1}{\sqrt{LC}} , \qquad F = \frac{R}{2L} , \qquad \omega_o \gg F ,$$

and

$$r_o(t) = e^{-\omega_F |t|} \tag{8.5}$$

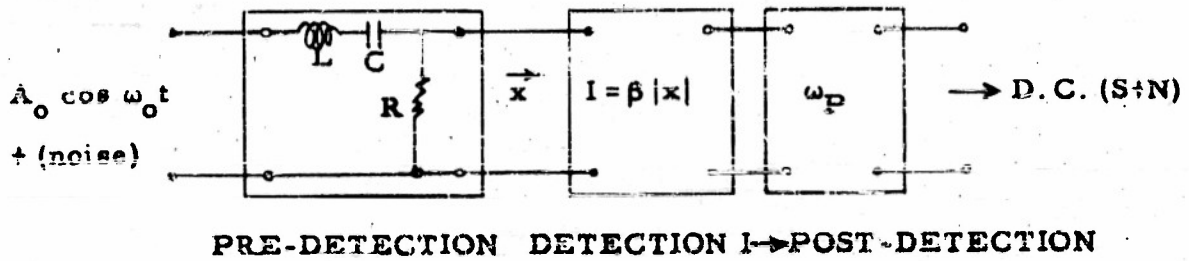

Fig. 26. Narrow-band noise and block diagram of detection system.

Writing $P_{s+n} = (S/N)^2$, we have

$$\left(\frac{2}{\pi} \frac{\omega_p}{\omega_F}\right) P_{s+n} = \frac{H(p)}{G(p)} \tag{8.6a}$$

where

$$H(p) = \left[{}_1F_1\left(-\frac{\nu}{2}; 1; -p\right) - 1\right]^2 \tag{8.6b}$$

$$G(p) = \sum_{m+n \neq 0} \frac{\left(-\frac{\nu}{2}\right)^2_{m+n} \; {}_1F_1\left(m+n-\frac{\nu}{2}; m+1; -p\right)^2 p^{m+n}}{n!\,(m!)^2\,(m+n)!\,(2n+m)} \tag{8.6c}$$

Since G(p) is a rather complicated function, various approximations have been developed for the extreme cases of weak and strong input signals ($p^2 \ll 1$, $p^2 \gg 1$).

A. Weak Signals

An approximation for G is developed in Appendix C for very small values of p, leading to an expression of the form

$$G(p) \doteq g_o(\nu) + g_1(\nu)\, p + g_2(\nu)\, p^2 \; . \tag{8.7}$$

From the general expression for ${}_1F_1$, a corresponding approximation for H(p) is:

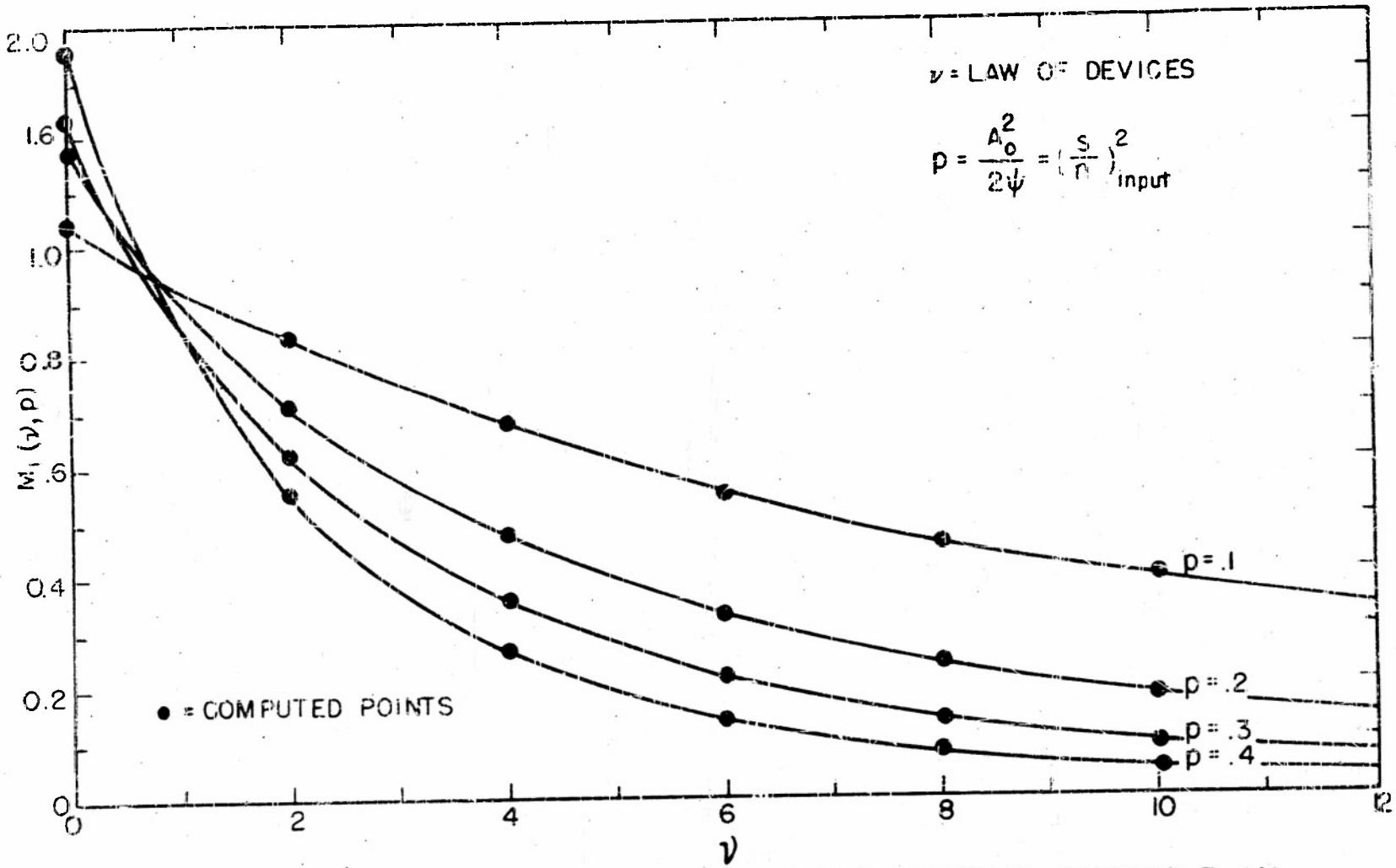

FIG. 27 THE FUNCTION M_1 FOR WEAK INPUT SIGNALS; SINEWAVE IN NARROW-BAND NOISE.

$$H(p) \doteq \left(\frac{\nu}{2}\right)^2 p^2 \left[1 + \frac{1}{2}\left(\frac{\nu}{2} - 1\right) p\right]^2 \quad . \tag{8.8}$$

Accordingly, P can be written

$$\left(\frac{2}{\pi}\,\frac{\omega_P}{\omega_F}\right) P_{s+n} \doteq M_1(\nu,p)\, Q_1(\nu)\, p^2 \quad ; \quad (p^2 \ll 1) \tag{8.9a}$$

where

$$Q_1 = \frac{\nu^2}{4 g_o(\nu)} \tag{8.9b}$$

is the function previously discussed (sec. 4), and $M_1(\nu,p)$ is a function which slightly modifies the shape of Q_1, according to the value of p. Thus, we have explicitly

$$M_1(\nu,p) = \left\{ \frac{1 + \left(\frac{\nu}{2} - 1\right) p + \frac{1}{4}\left(\frac{\nu}{2} - 1\right) p^2}{1 + \frac{g_1(\nu)}{g_o(\nu)}\, p + \frac{g_2(\nu)}{g_o(\nu)}\, p^2} \right\} \quad . \tag{8.10}$$

This function is plotted in Fig. 27. Note that as p increases, the function M_1 becomes sharper around $0 < \nu < 2$, and thereby tends to dampen out the slight maximum due to $Q_1(\nu)$. For extremely small p, $M(\nu,p)$ approaches unity, so that (8.9) becomes simply

$$\left(\frac{2}{\pi}\,\frac{\omega_P}{\omega_F}\right) P_{s+n} = Q_1(\nu)\, p^2 \quad , \quad (p^2 \to 0) \quad , \tag{8.10a}$$

which is exactly the expression (4.1) discussed in sec. 4E. The denominator of Q_1 contains an important term, $g_o(\nu)$, which is:

$$g_o(\nu) = \frac{1}{2} \sum_{n=1}^{\infty} \frac{\left(-\frac{\nu}{2}\right)^{2n}}{(n!)^2} \quad . \tag{8.11}$$

The function Q_1 is plotted in Figs. 12(a) and 12(b), respectively, with a db and direct numerical scale. Figure 12(a) is the same as Fig. (4.1) ref. 13, extended from $0 < \nu < 1$.

B. Strong Signal

In Appendix D the value of P_{s+n} is shown for large P to be:

$$\left(\frac{2}{\pi}\frac{\omega_P}{\omega_F}\right) P_{s+n} = \frac{2p}{\nu^2}\left\{\frac{L(\nu)^2 + \left(\frac{\nu}{2}\right)^2 L(\nu)\, p^{-1}}{1 + \frac{1}{4}\left[\frac{5}{2}\nu^2 - 5\nu - 1\right] p^{-1}}\right\} \qquad (8.12)$$

$$L(\nu) = \left[1 + p^{-\frac{\nu}{2}}\left(\frac{\nu}{2}+1\right)\right]$$

This has the form $Q_3(\nu)$, where Q_3 is described in sec. 4.

C. The Ideal Clipper

For this case $\nu = 0$, and when p is large, such a device possesses the greatest output signal-to-noise. From Appendix D we get

$$\left(\frac{2}{\pi}\frac{\omega_P}{\omega_F}\right) P_{s+n} = \frac{p(\ln p + 0.577)^2}{2} \qquad (8.13)$$

This last expression gives the departure from the simple dependence on p discussed in sec. 4.

D. Summary

Thus, from the approximation (8.9) for small p, from the exact expressions (8.6) for immediate values of p, and from (8.12) for large p, we obtain the entire dependence of P_{s+n} upon the input signal-to-noise ratio for various νth-law devices, as is shown in Fig. 19. If we are interested in P_{s+n} as a function of ν, with p as a parameter, then the variation shown in Fig. 20 is presented.

9. Narrow-band "Noise"-Signal in Narrow-band Noise

Analogous to sec. 8 we find from (7.43) the low-frequency correlation function $R(t)_c$, that the d-c terms appearing in the output signal indication are:

$$(W_{d.c.})_{N'|N} = C_\nu (1+p)^2 \qquad (9.1a)$$

$$(W_{d.c.})_N = C_\nu \ , \tag{9.1b}$$

so that the d-c increment is

$$S = \sqrt{C_\nu}\ [(1+p)^{\frac{\nu}{2}} - 1]. \tag{9.2}$$

The fluctuation noise intensity N^2 is

$$N^2 = C_\nu\ (1+p)^\nu \cdot I_\nu \ , \tag{9.3}$$

where I_ν is an integral obtained from $R(t)_o$ using the same correlation functions (8.5) for the narrow-band noise as were used in sec. 8: viz.:

$$I_\nu = \frac{2}{\pi}\,\omega_P \int_0^\infty [{}_2F_1(-\tfrac{\nu}{2}, -\tfrac{\nu}{2}; 1; e^{-2\omega_F t}) - 1]\ dt \ ,$$

$$= (\frac{2}{\pi}\,\frac{\omega_P}{\omega_F})\ g_o(\nu) \ . \tag{9.4}$$

[The function $g_o(\nu)$ has been previously defined in (8.11).] We have therefore

$$(\frac{2}{\pi}\,\frac{\omega_P}{\omega_F})\ P_{n'+n} = [\frac{1}{g_o(\nu)}][1 - (1+p)^{-\frac{\nu}{2}}]^2 \ . \tag{9.5}$$

A. Weak Signals

For small values of p we get

$$(\frac{2}{\pi}\,\frac{\omega_P}{\omega_F})\ P_{n'+n} \doteq [\frac{\nu^2}{4g_o(\nu)}]\ p^2 = Q_1(\nu)\ p^2 \ , \tag{9.6}$$

which is identical with eq. (8.10a) for a sinusoid in noise. Thus, for $p \ll 1$, we can write

$$P_{n'+n} = P_{s+n} \ .$$

B. Strong Signals

At the other extreme ($p^2 >> 1$) it is seen from (9.5) that

$$\lim_{\nu > 1,\, p \to \infty} \left[1 - (1+p)^{-\frac{\nu}{2}} \right]^2 = 1$$

so that for very large input ratios ($p \sim 20$ db) and $\nu \geq 1$, $P_{n'+n}$ is essentially independent of p and approaches

$$\left(\frac{2}{\pi} \frac{\omega_P}{\omega_F} \right) P_{n'+n} \simeq 1/g_o(\nu) = Q_5(\nu) \,, \qquad (9.8)$$

as was discussed in sec. 4. Q_5 is plotted in Fig. 28.

C. The Ideal Clipper

For the case of the ideal clipper ($\nu = 0$), we have

$$\left(\frac{2}{\pi} \frac{\omega_P}{\omega_F} \right) P_{n'+n} = \rho^2 Q_1(0)\, M_2(0,\rho)$$

$$Q_1(0) = 1.6715$$

$$M_2(0,\rho) = 1 \,.$$

Thus,

$$\left(\frac{2}{\pi} \frac{\omega_P}{\omega_F} \right) P_{n'+n} = 1.6715 \left[\ln(1+p) \right]^2 . \qquad (9.9)$$

D. Summary

The dependence of $P_{n'+n}$ on p for a particular device is plotted over the entire range of values of p, with ν as a parameter: for small p, with the help of the approximation (9.6); intermediate p from the exact expression (9.5), and large p, from the approximation (9.8). The complete functional dependence is shown in Fig. 21.

We may investigate the dependence of $P_{n'+n}$ on ν, more thoroughly for this case [1(b)] than for case 1(a) sec. 8A, since (9.5) is more

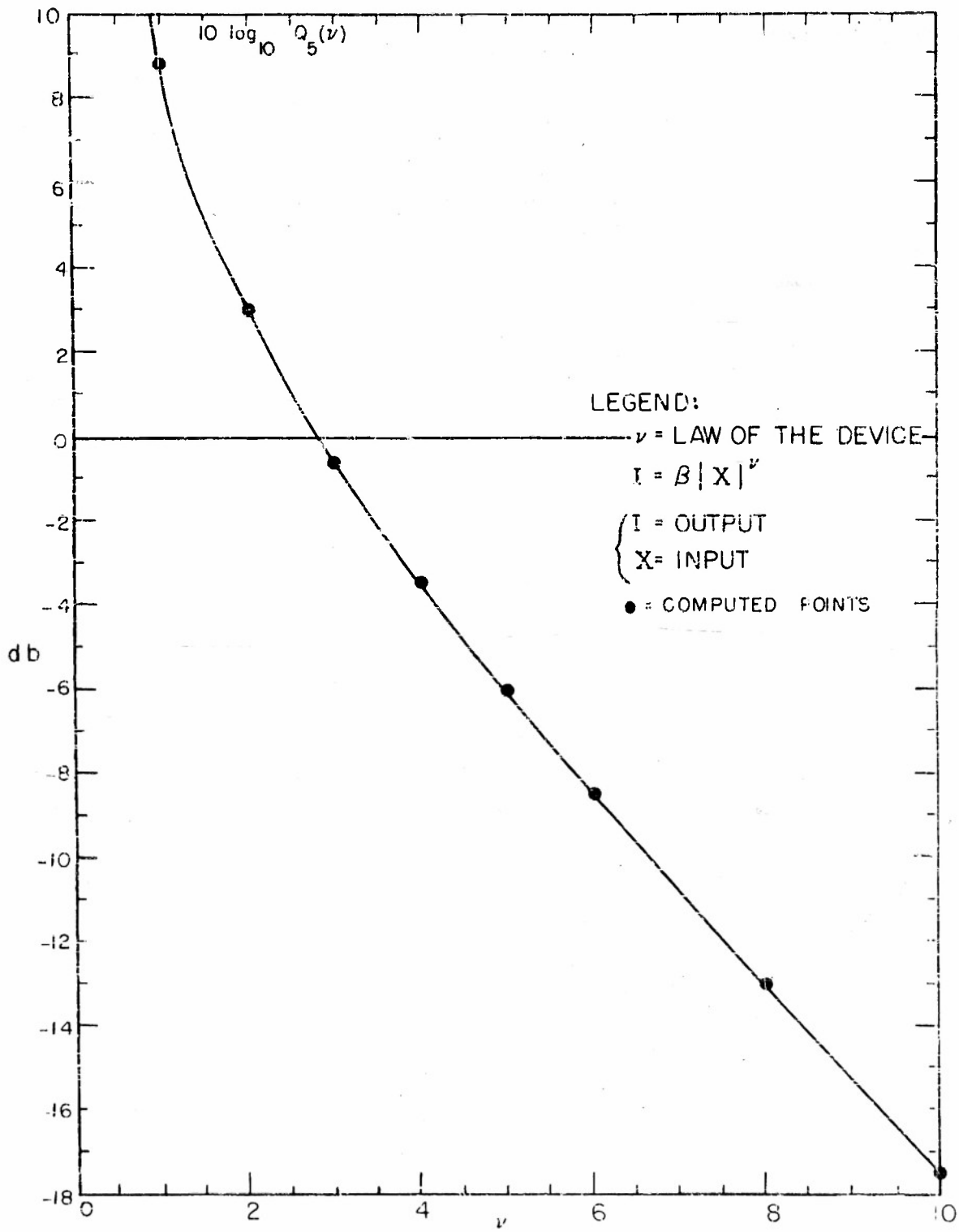

FIG. 28 OUTPUT (S/N) VS. DETECTOR LAW FOR VERY LARGE INPUT RATIO. INPUT: NARROW-BAND "NOISE"-SIGNAL IN NARROW-BAND NOISE.

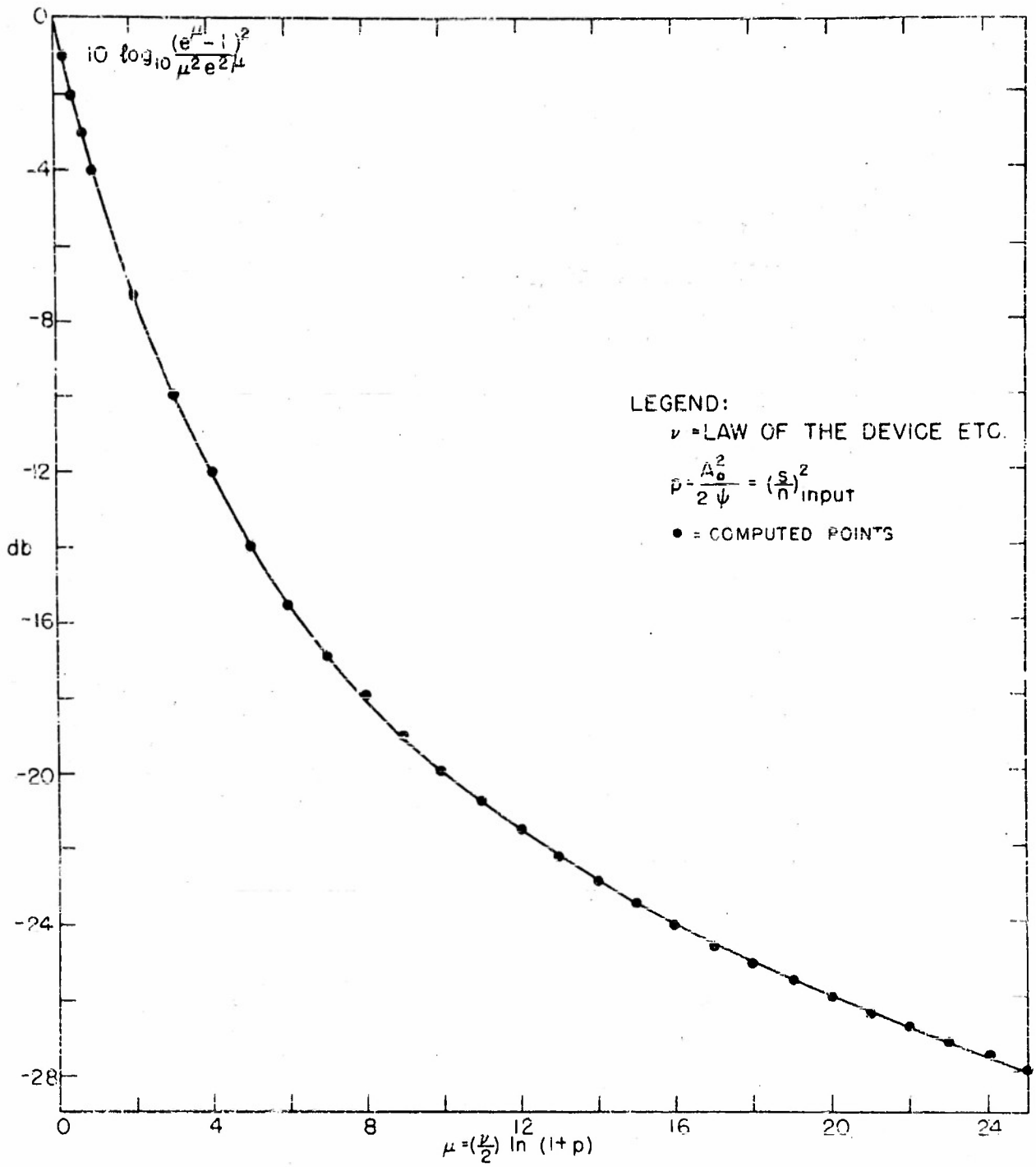

FIG. 29 M_2 AS A FUNCTION OF $\mu = (\frac{\nu}{2}) \ln (1+p)$, DESCRIBING THE EFFECT OF INPUT (S/n) ON Q_1 (ν).

amenable to exact treatment than (8.6a).

Let us define a new variable ρ such that:

$$\rho = \ln (1+p) \; ; \tag{9.10}$$

then the exact expression for $P_{n'+n}$ (9.5) can be re-expressed as

$$\left(\frac{2}{\pi} \frac{\omega P}{\omega_F}\right) P_{n'+n} = \rho^2 Q_1(\nu)\, M_2(\nu, p) \; , \tag{9.11}$$

where

$$M_2(\nu, p) = \frac{(e^{u} - 1)^2}{u^2 e^{2u}} \quad , \tag{9.11a}$$

$$u = \left(\frac{\nu}{2}\right) \rho = \left(\frac{\nu}{2}\right) \ln (1+p) \; . \tag{9.11b}$$

We have the rather elegant result that the output $P_{n'+n}$ appears as a product of three function, each of whose behavior we can determine easily. The first (ρ^2) is a scale factor depending on the input signal-to-noise ratio. For small p, $\rho^2 \rightarrow p^2$, M_2 is constant and equal to 1 over the range of interest in ν, so that the behavior (9.6) for low input (s/n) is preserved. $Q_1(\nu)$ is the by-now familiar relation shown in Figs. 12(a) and 12(b), which describe the behavior of various νth-law devices at low input signal-to-noise levels. It is fortunate that M_2 is a simple function of a single variable, u, [cf. (9.11b)]. The function M_2 is shown in Fig. 29. We see that M_2 has the same general shape as the curves of M_1 (Fig. 27), is M_2 is plotted vs. ν, p as parameter. For increasing values of p, the very "sharp" behavior of M_2 in the region $0<u<4$ tends to dominate the small maximum in $Q_1(\nu)$, as can be seen by a simple addition of decibels in Figs. 29 and 12(a), when p is large. This acts to make the maximum of Q_1 disappear, and the characteristic "peaked" behavior of M_2 near $\nu = 0$ is typical of the function $P_{n'+n}$. The function M_2 explains the disappearance of the signal-to-noise maximum of $P_{n'+n}$ versus ν at large input.

Again for threshold signals, the maxima of the product $Q_1 M_2$ tend to disappear rather rapidly. Therefore, with (9.11) for $P_{n'+n}$, an approxi-

mation has been developed for the locus of $(P_{n'+n})_{max}$ in the ν-p-plane. The details are left to Appendix E; the results are shown in Fig. 30. Finally, the dependence of $P_{n'+n}$ on ν for a given input (signal-to-noise) is shown in Fig. 22, which effectively summarizes the above remarks.

10. Sinusoidal Signal and Broad-band Noise

It was noted in sec. 7C that the output correlation function (7.21) can be written:

$$R(t) = \sum_{n+m=2\ell}^{\infty} \left[\frac{4 H_{mn}^2 \epsilon_m \psi^n}{n!} \right] \left[r(t)^n \cos m\omega_o t \right]$$

$$= \sum_{\ell=1,2,\ldots} C_{mn} \left[r(t)^n \cos m\omega_o t \right] \qquad (10.1)$$

where the H_{mn} have been evaluated (7.31). It was also observed in sec. 7D that the d-c voltage increment S is independent of the spectral structure of the noise, leaving the value

$$S = 2[H_{oo} - h_{oo}] = \sqrt{C_\nu} \left[{}_1F_1\left(-\frac{\nu}{2}, \quad ; 1; -p\right) - 1 \right],$$

from eqs. (7.25) and (8.1). Part of our problem, therefore, in obtaining P_{s+n} is to compute the band-structure factor

$$4 T_{mn} = 4 \int_o^\infty r(t)^n \cos m\omega_o t \; dt \;,$$

which is needed in

$$W(C) = 4 \int_o^\infty R'(t) \; dt.$$

A convenient spectral model is provided by the so-called "optical" spectrum whose correlation function is

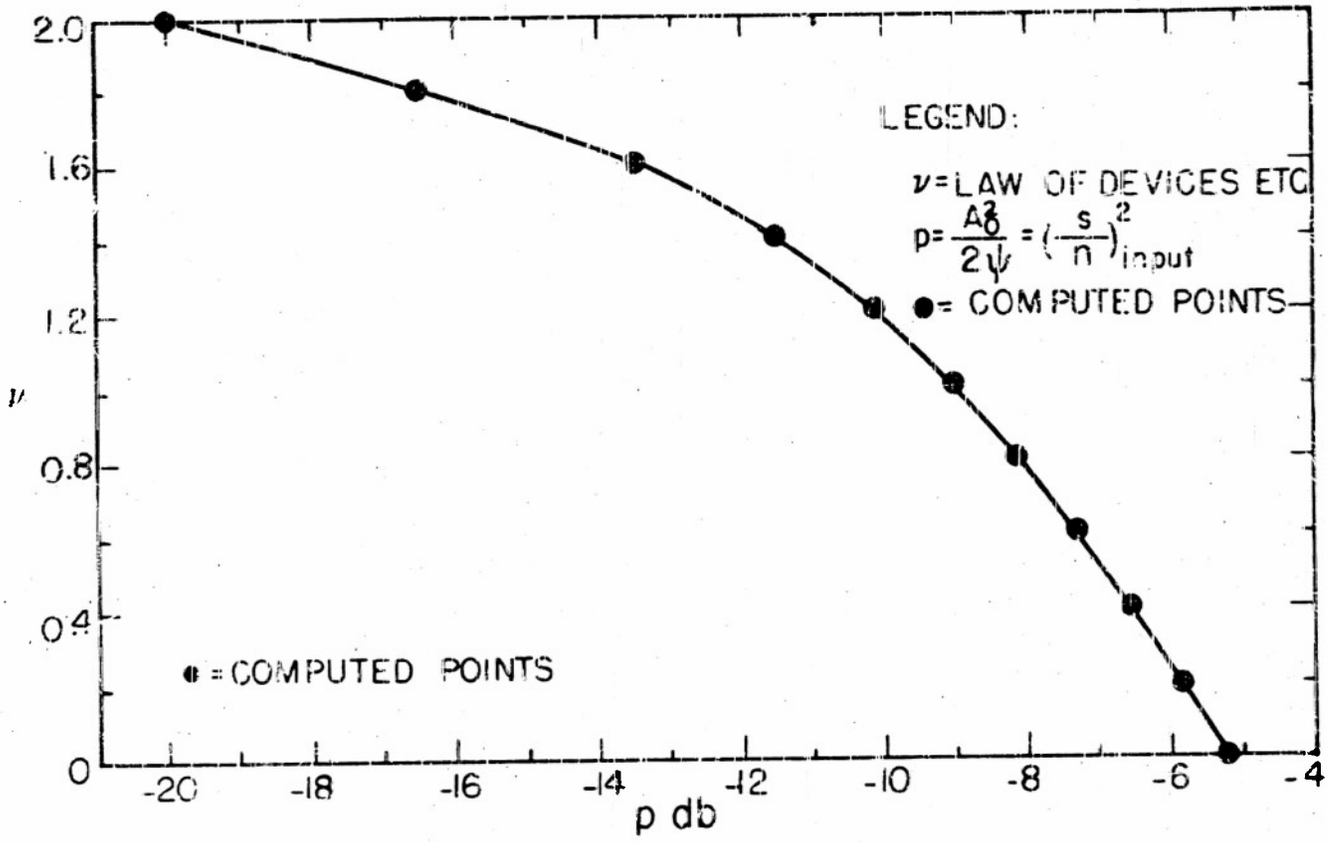

FIG.30 LOCUS OF $(P_{n'+n})$ max.

$$r(t) = e^{-\omega_F |t|} \quad . \tag{10.2}$$

From this we find that

$$4T_{mn} = \frac{4n\omega_F}{(n\omega_F)^2 + (m\omega_o)^2} \quad . \tag{10.3}$$

[Observe that T_{11}, with ω replacing ω_o, is the normalized* power spectrum of the input; i.e.,

$$w(f) = 4\int_o^\infty r(t)\cos \omega t \; dt \quad .]$$

For the "normalized" spectrum explicitly one has

$$w(f) = 4\,\omega_F/(\omega_F^2 + \omega^2) \tag{10.4}$$

as sketched in Fig. 31.

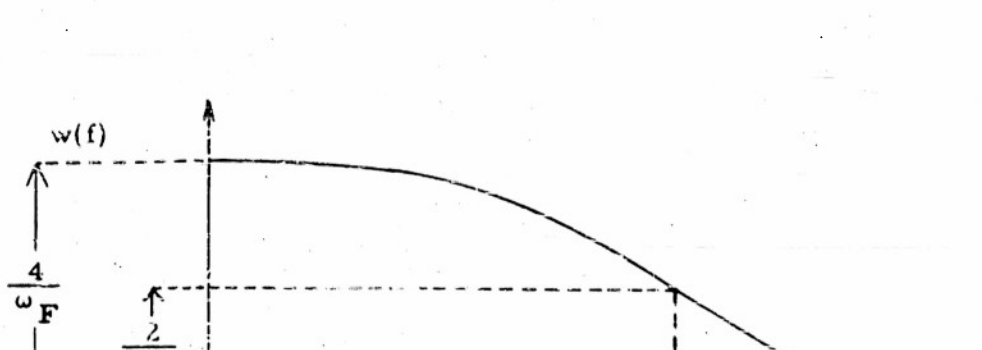

Fig. 31. A normalized power spectrum of input noise: "Optical Spectrum."

*i.e. spectrum corresponding to the normalized auto-correlation function r(t).

When $\omega = \omega_F$, $w(f_F) = w(0)/2$, the value at the half-power point; ω_F is the (angular) "bandwidth" of the input noise.

Expressing the signal frequency as

$$\omega_o = k\,\omega_F \quad , \tag{10.5}$$

we can rewrite T_{mn} as

$$T_{mn} = \frac{1}{\omega_F}\,\frac{n}{n^2 + (km)^2} \quad . \tag{10.6}$$

Another useful model for the background noise of the spectrum is the gaussian response, whose normalized correlation function is

$$r(t) = e^{-a^2 t^2} \quad . \tag{10.7}$$

Consequently, we have

$$4T_{mn} = \frac{2}{a}\sqrt{\frac{\pi}{n}}\; e^{-\left(\frac{\omega_o}{a}\right)^2 \frac{m^2}{4n}} \quad . \tag{10.8}$$

The normalized power spectrum $w(f)$ is

$$w(f) = 4T_{11}(\omega) = \frac{2\sqrt{\pi}}{a}\; e^{-\frac{\omega^2}{4a^2}} \quad . \tag{10.9}$$

The half-power point occurs when

$$\omega = \omega_F = 1.77\,a \quad . \tag{10.10}$$

Thus we designate the location of the half-power point as the pre-detection bandwidth of the background noise ω_F, (cf. (10.10)). In terms of ω_F the normalized input spectrum is:

$$w(f) = \frac{1}{\omega_F}\,(1.77 \times 2\sqrt{\pi})\; e^{-\frac{1}{4}\left(\frac{1.77\,\omega}{\omega_F}\right)^2} \quad . \tag{10.11}$$

Similarly: $$T_{mn} = \frac{1}{\omega_F}\left(\frac{1.77\sqrt{\pi}}{2\sqrt{n}}\right) e^{-(1.77k)^2 \frac{m^2}{4n}} . \qquad (10.12)$$

Attention is now turned to the calculation of $(S/N)_{out}$: The output noise intensity N^2 is

$$N^2 = 4f_p \sum_{\ell=1} C_{mn} T_{mn} = \left(\frac{2}{\pi}\frac{\omega_p}{\omega_F}\right) \sum_{\ell=1} C_{mn}(\omega_F T_{mn}) , \qquad (10.13)$$

and since

$$P_{s+n} = (S/N)^2 ,$$

we can write

$$\left(\frac{2}{\pi}\frac{\omega_p}{\omega_F}\right) P_{s+n} = \left[{}_1F_1\left(-\frac{\nu}{2}; 1; -p\right) - 1\right]^2 \Big/ \sum_{\substack{\ell=1 \\ m+n=2\ell}} \left[\frac{C_{mn}}{C_\nu}\right](\omega_F T_{mn}) ; \qquad (10.14)$$

C_{mn}/C_ν has been calculated for the νth-law detector, and is found to be from (7.31):

$$\frac{C_{mn}}{C_\nu} = \epsilon_m \left[\frac{p^m}{(m!)^2}\right]\left[\frac{2^n}{n!}\right]\left[\frac{\Gamma\left(\frac{\nu}{2}+1\right)}{\Gamma\left(\frac{\nu}{2}+1-\ell\right)}\right]^2 {}_1F_1\left(\ell - \frac{\nu}{2}; m+1; -p\right)\Big]^2 . \qquad (10.15)$$

Then, as in sec. 8 P_{s+n} is

$$\left(\frac{2}{\pi}\frac{\omega_p}{\omega_F}\right) P_{s+n} = H(p)/G'(p) . \qquad (10.16)$$

Approximations with respect to p are independent of the band-structure factor T_{mn}, and depend only on H_{mn}^2 in C_{mn}; thus, our results will be given in terms of $(\omega_F T_{mn})$.

A. Weak Signals

As before, for small p, G'(p) can be written as a power series,

$$G'(p) = g'_o(\nu) + g'_1(\nu)\, p + g'_2(\nu)\, p^2 . \qquad (10.17)$$

All terms except $g'_o(\nu)$ depend on k. The general behavior of the function for this case is the same as in sections 8A and 9B; the discussion of section 4 applies here also. The first term $g'_o(\nu)$ has been evaluated in Appendix F. Neglecting the terms in $g'_i(\nu)$, i>1, we write

$$\left(\frac{2}{\pi}\frac{\omega}{\omega}\frac{P}{F}\right) P_{s+n} = \left[\frac{\nu^2}{4 g'_o(\nu)}\right] p^2 = Q_2(\nu)\, p^2 , \qquad (10.18)$$

where
$$g'_o(\nu) = \sum_{n=1}^{\infty} \frac{\left(-\frac{\nu}{2}\right)^2_n}{\left(\frac{1}{2}\right)_n n!} \left(\omega_F T_{0,2n}\right) . \qquad (10.19)$$

Thus, for the "optical" spectrum we have

$$g'_o(\nu) = \sqrt{\pi} \sum_{n=1}^{\infty} \frac{\left(-\frac{\nu}{2}\right)^2_n}{\Gamma\left(n+\frac{1}{2}\right) n!} \frac{1}{2n} \qquad (10.20)$$

and for the Gauss spectrum :

$$g'_o(\nu) = \left[\frac{(1.77)\,\pi}{2}\right] \sum_{n=1}^{\infty} \frac{\left(-\frac{\nu}{2}\right)^2_n}{\Gamma\left(n+\frac{1}{2}\right) n!} \frac{1}{\sqrt{2n}} . \qquad (10.21)$$

These expressions are to be compared with

$$g'_o(\nu) = \sum_{n=1}^{\infty} \frac{\left(-\frac{\nu}{2}\right)^2_n}{\Gamma(n+1) n!} \frac{1}{2n} , \qquad (10.22)$$

which suggests why the shape of the two curves for Q_1 and Q_2 are similar. Notice that Q_2 is independent of the spectral location of the sinusoid in the noise. For the optical spectrum, we have explicitly

$$Q_2(\nu)_{opt.} = \frac{\nu^2}{\sqrt{\pi} \sum_{n=1}^{\infty} \frac{(-\frac{\nu}{2})_n^2}{\Gamma(n+\frac{1}{2})n!(2n)}} \tag{10.23}$$

and for the gauss spectrum this becomes

$$Q_2(\nu)_{gauss.} = \frac{\nu^2}{(1.77 \times 2\pi) \sum_{n=1}^{\infty} \frac{(-\frac{\nu}{2})_n^2}{\Gamma(n+\frac{1}{2})n! \sqrt{2n}}} \tag{10.24}$$

Figures 13 and 14 illustrate (10.23), (10.24).

B. Strong Signals

For large values of the input signal-to-noise ratio, we have calculated expressions (cf. Appendix G) which, when not in the clipping region ($\nu < 1$), may be reduced to

$$(\frac{2}{\pi}\frac{\omega_P}{\omega_F})\, P_{s+n} = Q_4(\nu)\, p, \qquad \nu > 1 \tag{10.25}$$

where

$$Q_4(\nu) = 1/\nu^2\, (\omega_F T_{11})$$

For the "optical" case we get

$$Q_4(\nu)_{opt.} = 1/\nu^2 \tag{10.26}$$

since $(\omega_F T_{11}) = 1$. For the gauss spectrum

$$Q_4(\nu)_{gauss} = (2/1.77\sqrt{\pi})\frac{1}{\nu^2} \tag{10.27}$$

The next order of approximation is summarized by

$$\frac{1}{Q_4(\nu)} = \nu^2[(\omega_F T_{11}) + [\nu(\frac{\nu}{2} - 1)\omega_F \Gamma_{11} + \frac{\nu^2}{8}(\omega_F T_{02}) + (\frac{\nu}{2} - 1)\omega_F T_{22}]\, p^{-1}] \tag{10.28}$$

which is valid part of the way into the clipping region ($\nu < 1$).

C. The Ideal Clipper

The important case of the super-clipping ($\nu = 0$), is determined in Appendix G, when $p^2 >> 1$.

$$\left(\frac{2}{\pi}\frac{\omega_p}{\omega_F}\right) P_{s+n} = p\,\frac{(\ln p + \gamma)^2}{4}\left(\frac{1}{\omega_F \frac{\pi}{11}}\right), \quad (p^2 >> 1) \qquad (10.29)$$

where γ is the Euler number, $\gamma = 0.577$. For particular background spectra, we use the results of (10.26) and (10.27), so that for an optical spectrum:

$$\left(\frac{2}{\pi}\frac{\omega_p}{\omega_F}\right) P_{s+n} = \frac{(\ln + \gamma)^2}{4}\, p, \qquad p >> 1 \qquad (10.30)$$

and for the Gauss spectrum:

$$\left(\frac{2}{\pi}\frac{\omega_p}{\omega_F}\right) P_{s+n} = \frac{1}{1.77\sqrt{\pi}}\,\frac{(\ln p + \gamma)^2}{2}\, p, \quad p >> 1. \qquad (10.31)$$

It is possible now, as before, to plot P_{s+n} as a function of p, for various νth-law detectors, with the help of (10.18) for low-input levels; the exact expression, (10.14) for intermediate values of p, and (10.25) for large input ratios. The class of spectrum chosen for calculation is the gauss, with

$$k = 1/1.77 .$$

This value of k corresponds to $\omega_o = \alpha$, or the case where the sine signal is at that part of the input power noise spectrum where the intensity is 0.788 w(0). The results of this calculation are summarized in Fig. 23, where

$$\omega_F T_{mn} = \frac{1.77\sqrt{\pi}}{2}\, e^{-\frac{m^2}{4n}}.$$

Again, curves of P_{s+n} are provided for constant p, and variable ν, and are presented in Fig. 24.

APPENDIX A

Expansion of W_2 in Terms of Hermite Functions

The development of W_2 in Hermite functions requires first the Fourier transform of W_2. Part of this is expanded in a power series, containing the correlation function; and then the inverse transform is taken, giving us once again W_2. For normal random noise ($V = 0$), the characteristic function is

$$F_2 = \exp\left[-\frac{\psi}{2}(\xi_1^2 + \xi_2^2 + 2\xi_1\xi_2 r(t))\right] = F(W_2) \qquad (A1)$$

(ref. 1, eq. (2.16)). Expanding F_2 as a power series in terms of the input correlation function, r, gives

$$F_2(\xi_1, \xi_2; t) = \sum_{k=0}^{\infty} \frac{r(t)^k}{k!} \left(\psi^{\frac{k}{2}} \xi_1^k e^{-\frac{\psi}{2}\xi_1^2}\right)\left(\psi^{\frac{k}{2}} \xi_2^k e^{-\frac{\psi}{2}\xi_2^2}\right) . \qquad (A2)$$

The inverse (complex) Fourier transformation is

$$G_2(X_1, X_2; t) = \frac{1}{4\pi^2} \int_{\underline{C}_1} d\xi_1 \int_{\underline{C}_2} d\xi_2 \, F_2(\xi_1, \xi_2; t) \exp -i[\xi_1 X_1 + \xi_2 X_2]. \qquad (A3)$$

In general, $\underline{C}$ is the contour, shown in Fig. 25, in the complex ξ-plane. Here, however, $\underline{C}$ extends along the entire real axis, and so $G_2 = W_2(X_1, X_2; t)$. Thus we have

$$W_2 = \frac{1}{\psi} \sum_{k=0}^{\infty} \frac{[-r(t)]^k}{k!} I_k , \qquad (A4)$$

$$I_k = (-1)^k \left\{ [C_k(X_1) C_k(X_2) - S_k(X_2)] - i [S_k(X_1) C_k(X_2) + C_k(X_1) S_k(X_2)] \right\} . \qquad (A5)$$

From considerations of symmetry of the terms in $\xi^k \cos X\xi$ and $\xi^k \sin X\xi$ we note that C_k is different from zero for $k = 2m$ only, and S_k exists for

$k = 2m + 1$ only. The imaginary terms go out, as was to be expected, since the original function W_2 is real. From eq. (A3.5) of ref. 1, we have for the even terms, $(k = 2m)$:

$$C_k(X) = \frac{2\psi^{m+\frac{1}{2}}}{2\pi} \int_0^{\infty} \xi^{2m} \cos X\xi \, e^{-\frac{\psi}{2}\xi^2} d\xi = (-1)^m \phi^{(2m)}\left(\frac{X}{\sqrt{\psi}}\right) \quad (A6)$$

where $\phi^{(2m)}$ is the Hermite function, $\phi^{(n)} = \frac{1}{\sqrt{2\pi}} \frac{d^n}{dx^n} e^{-\frac{x^2}{2}}$.

For the odd terms, $(k = 2m + 1)$ we get

$$S_k(X) = \frac{2\psi^{m+1}}{2\pi} \int_0^{\infty} \xi^{2m+1} \sin X\xi \, e^{-\frac{\psi}{2}\xi^2} d\xi = (-1)^{m+1} \phi^{(2m+1)}\left(\frac{X}{\sqrt{\psi}}\right). \quad (A7)$$

Thus,

$$I_{2m} = \phi^{(2m)}\left(\frac{X_1}{\sqrt{\psi}}\right) \phi^{(2m)}\left(\frac{X_2}{\sqrt{\psi}}\right) \quad (A8a)$$

$$I_{2m+1} = \phi^{(2m+1)}\left(\frac{X_1}{\sqrt{\psi}}\right) \phi^{(2m+1)}\left(\frac{X_2}{\sqrt{\psi}}\right) \quad (A8b)$$

and therefore we can write

$$W_2(X_1, X_2; t) = \frac{1}{\psi} \sum_{k=0}^{\infty} \frac{[-r(t)]^k}{k!} \phi^{(k)}\left(\frac{X_1}{\sqrt{\psi}}\right) \phi^{(k)}\left(\frac{X_2}{\sqrt{\psi}}\right). \quad (A9)$$

For $t = 0$, W_2 is a δ-function, $\delta(X_1 - 0, X_2 - 0)$, so that the expansion is not valid for this value of t.

APPENDIX B

The Calculation of R(t) Directly from W_2

Here we have for the amplitude functions

$$h_{o,k} = \beta [4\psi^{k+1}]^{\frac{1}{2}} L_k \tag{B1}$$

$$L_k = \int_{-\infty}^{\infty} |X|^{\nu} \phi^k (X/\sqrt{\psi}) \, dX \tag{B2}$$

with,

$$\phi^{(2m+1)}(\mu) = -\phi^{(2m+1)}(-\mu) \; ; \; \phi^{2m}(\mu) = \phi^{2m}(-\mu) \, ,$$

from the integral definitions of the Hermite functions (App. A).

Hence, by the symmetry properties of the integrand,

$$L_{2m+1} = 0 \, , \text{ and}$$

$$\left\{ L_{2m} = 2 \int_o^{\infty} X^{\nu} \phi^{2m} \left(\frac{X}{\sqrt{\psi}} \right) dX = 2C \int_o^{\infty} X^{\nu} \, {}_1F_1 \left(-m; \frac{1}{2}; \frac{X^2}{2\psi} \right) dX \right\} \tag{B3}$$

from ref. 1, (A3.9). The constant C is specifically

$$C = \frac{1}{\sqrt{2\pi}} (-1)^m \frac{(2m)!}{2^m m!} \, . \tag{B4}$$

To evaluate the integral, we choose a typical term

$$\int_o^{\infty} X^{2k+\nu} e^{-\frac{X^2}{2\psi}} dX = \frac{(2\psi)^k}{2} (2\psi)^{\frac{\nu+1}{2}} \Gamma \left(\frac{\nu+1}{2} \right) \left(\frac{\nu+1}{2} \right)_k \, .$$

We have

$$L_{2m} = C\left[(2\psi)^{\frac{\nu+1}{2}}\Gamma\left(\frac{\nu+1}{2}\right)\right]\sum \qquad \text{(B5)}$$

with

$$\sum = \sum_{k=0}^{\infty} \frac{(-m)_k \left(\frac{\nu+1}{2}\right)_k}{\left(\frac{1}{2}\right)_k} \frac{1}{k!} = {}_2F_1\left(-m, \frac{\nu+1}{2}; \frac{1}{2}; 1\right)$$

(cf. section 6(A) for the definition of ${}_2F_1$). The value of $\sum$ is

$$\sum = \Gamma\left(\frac{1}{2}\right)\Gamma\left(m-\frac{\nu}{2}\right)/\Gamma\left(-\frac{\nu}{2}\right)\Gamma\left(m+\frac{1}{2}\right) = \left(-\frac{\nu}{2}\right)_m / \left(\frac{1}{2}\right)_m$$

from the relationship (ref. 1, A3.20(a)):

$${}_2F_1(\alpha,\beta;\gamma;1) = \Gamma(\gamma)\Gamma(\gamma-\alpha-\beta)/\Gamma(\gamma-\alpha)\Gamma(\gamma-\beta);\ \mathrm{Re}(\gamma-\alpha-\beta) > 0\ .$$

Hence, we can write

$$4\left[\frac{\psi^{2m}}{(2m)!}\right] h_{o,2m}^2 = \left[\frac{\beta^2}{\pi}\Gamma\left(\frac{\nu+1}{2}\right)^2 (2\psi)^{\nu}\right]\left[\frac{\left(-\frac{\nu}{2}\right)_m^2}{\left(\frac{1}{2}\right)_m m!}\right]\left[\frac{(2m)!}{m!}\ \frac{1}{2^{2m}\left(\frac{1}{2}\right)_m}\right]. \qquad \text{(B6)}$$

The last factor is unity, since

$$\frac{(2m)!}{m!} = 2^{2m}\cdot\frac{\Gamma\left(\frac{1}{2}\right)}{\sqrt{\pi}}\cdot\left(\frac{1}{2}\right)_m = 2^{2m}\left(\frac{1}{2}\right)_m .$$

Thus, we have for the correlation function

$$R(t) = \sum_{m=0}^{\infty} r(t)^{2m}\, 4\left[\frac{\psi^{2m}}{2m!}\right] h_{0,2m}^2$$

$$= C_{\nu}\ {}_2F_1\left(-\frac{\nu}{2}, -\frac{\nu}{2}; \frac{1}{2}; r(t)^2\right)\ . \qquad \text{(B7)}$$

where

$$C_\nu = \frac{(2\psi)^2}{\pi}\left\{\frac{\Gamma(\frac{\nu+1}{2})}{\Gamma(\frac{\nu}{2})}\right\}^2 \qquad (B8)$$

APPENDIX C

Calculation of G(p) for Small Input (s/n)

We want G(p) in the form

$$G(p) \doteq g_o(\nu) + g_1(\nu)\, p + g_2(\nu)\, p^2 \qquad (C1)$$

Using the terminated series representing ${}_1F_1$,

$${}_1F_1(\alpha;\beta\ ;\ -p) = \left[1 - \frac{\alpha}{\beta}\, p + \frac{\alpha(\alpha+1)}{\beta\,(\beta+1)}\,\frac{p^2}{2}\right] \qquad (C2)$$

we find that

$$\left.\begin{aligned} g_o(\nu) &= \sum_{n=1}^{\infty}{}' b_n \\ g_1(\nu) &= 2\sum_{n=1}^{\infty}{}' (N\, b_n - n b_n) + 2\sum_{n=0}^{\infty}{}' C_n \\ g_2(\nu) &= \sum_{n=1}^{\infty}{}' \frac{3}{2}\, n^2\, b_n + (\tfrac{1}{2} - 3N)\, n b_n + \tfrac{N}{2}(3N-1)\, b_n + 2\sum_{n=0}^{\infty}{}' (N-1)\, C_n - n C_n \\ &\quad + \frac{1}{2}\sum_{n=0}^{\infty}{}' d_n \end{aligned}\right\} \qquad (C3)$$

where

$$N = \frac{\nu}{2}\ , \text{ and} \qquad (C4a)$$

$$b_n = \frac{(-N)_n^2}{n!\,n!\,(2n)}\ ; \quad C_n = \frac{(-N)_{n+1}^2}{n!\,(n+1)!\,(2n+1)}\ ; \quad d_n = \frac{(-N)_{n+2}^2}{n!\,(n+2)!\,(2n+2)} \qquad (C4b)$$

Define the quantities:

$$\sum_{n=1}^{\infty} b_n = g_o(N)$$

$$\frac{\Gamma(2N+1)}{\Gamma(N+1)^2} - 1 = F_1(N)$$

$$\frac{\Gamma(2N)}{\Gamma(N+1)^2} - 1 = F_2(N) \qquad \text{(C5)}$$

$$\sum_{n=0}^{m} C_n = F_3(N)$$

$$\sum_{n=1}^{\infty} n\, C_n = F_4(N)$$

Then we find:

$$\sum_{n=1} n\, b_n = F_1(N)/2$$

$$\sum_{n=1} n^2 b_n = \frac{N^2}{2}(F_2+1) \qquad \text{(C6)}$$

$$\sum_{n=0} d_n = \frac{N^2}{2} F_2 \ .$$

Consequently, we can write

$$g_1(\nu) = N[2g_o(N)] - F_1 + 2F_3 \qquad \text{(C7)}$$

$$g_2(\nu) = \frac{N}{4}(3N-1)[2g_o(N)] + \frac{1}{2}\left(\frac{1}{2} - 3N\right)F_1 + N^2F_2 + 2(N-1)F_3 - F_4 + \frac{3}{4}N^2.$$

APPENDIX D

Calculation of $(P_{s+n})_{N.B.}$ for Strong Signals

As in Appendix C, we write

$$N = \frac{\nu}{2}, \tag{D1}$$

We use the assymptotic expansion for ${}_1F_1$ [ref.5, eq. (A3.3)] :

$${}_1F_1(a;\beta;-x) \simeq \frac{\Gamma(\beta)}{\Gamma(\beta-a)}\, x^{-a}\left[1 + \frac{a(a-\beta+1)}{x\,1!} + \frac{a(a+1)(a-\beta+1)(a-\beta+2)}{x^2\,2!} + \cdots\right].$$

For the numerator of P_{s+n} then,

$$H(p) = \left[{}_1F_1(-N;\,1;\,-p) - 1\right]^2 = \frac{p^{2N}}{\Gamma(N+1)^2}\; Z(N,p) \tag{D2}$$

where $Z(N,p) = L(N)^2 + L(N)\,N^2 p^{-1} + \left[L(N)\,N^2(N+1)^2 + N^4\right] p^{-2}$ (D3)

and

$$L(N) = \left[1 + \Gamma(N+1)\, p^{-N}\right], \tag{D4}$$

For the denominator G(p) we use

$${}_1F_1(m+n-N;\,m+1;\,-p)^2 = \frac{m!}{\Gamma(N+1-n)^2}\; p^{-2(m+n)}\, p^{2N}\, f_{mn}(p) \tag{D5}$$

where

$$f_{mn}(p) = \left\{1 + 2(N-n)(N-n-m)\,p^{-1}\right\} + (N-n)(N-m-n)$$

$$\left[2(N-n-1)(N-m-n) - 4(N-m-n) - m + 1\right] p^{-2}.$$

Thus,

$$\frac{H(p)}{G(p)} = \frac{p\, Z(N,p)}{\sum_{m,n} p^{1-n-2n}\, C'_{mn}\, f_{mn}} \tag{D7}$$

where $C'_{mn} = \frac{\epsilon_m (-N)^2_{m+n} (N+1-n)^2_n}{n!(m+n)!(m+2n)}$; from $\frac{\Gamma(N+1)}{\Gamma(N+1-n)} = (N+1-n)_n$. (D8)

Thus, using C'_{10}, C'_{20}, C'_{01}, and C'_{30}, with the corresponding f_{mn}:

$$\frac{H(p)}{G(p)} = \frac{p}{2N^2} \frac{Z(N,p)}{Y(N,p)} \tag{D9}$$

$$Y(N,p) = 1 + \frac{1}{4}(10N^2 - 10N - 1)p^{-1} + \frac{(N-1)^2}{18}(58N^2 - 128N+4)p^{-2} \tag{D10}$$

Including terms only in p^{-1} in Y and z, P_{s+n} is then

$$\frac{H}{G} = \frac{p}{2N^2}\left\{\frac{L(N)^2 + N^2 L(N) p^{-1}}{1 + \frac{1}{4}(10N^2 - 10N - 1)p^{-1}}\right\} \tag{D11}$$

which holds part of the way into the clipping region ($v < 1$).

For the ideal clipper, $N \longrightarrow 0$, so that we have

$$L(N) \longrightarrow N(\ln p + \gamma)$$

from

$$p^{-N} = e^{-N \ln p} \simeq 1 - N \ln p + \ldots$$

and

$$\Gamma(N+1) = \Gamma(0) + N\Gamma'(0) = 1 + N\gamma ,$$

$$\gamma = 0.5772\ldots, \text{ Euler's number.}$$

In this case,

$$H(p)/G(p) \simeq \frac{p}{2}(\ln p + \gamma)^2 / [1 - \frac{1}{4}p^{-1} + \ldots] \simeq \frac{p}{2}(\ln p + \gamma)^2 \tag{D12}$$

APPENDIX E

Calculation of the Locus of $(P_{n'+n})_{max}$ in the ν-p-plane

We substitute $N = \nu/2$ in the expression for $P_{n'+n}$, so that we find that the condition for a maximum of $P_{n'+n}$ as a function of N, (in the ν-p-plane), is determined by the condition,

$$\frac{dP_{n'+n}}{dN} = 0 \quad . \qquad \left(\frac{d^2P}{dN^2} < 0\right) \quad , \tag{E1}$$

where $$P_{n'+n} = \rho^2 Q_1(N)\, M_2(N,p), \quad \text{from} \tag{9.11}$$

In the region in which we are interested, $Q_1(N)$ may be approximated by a parabola, [from Fig. 12(b)],

$$Q_1(N) = [2 - k(N-1)^2] \tag{E2}$$

with $$k = 0.33 \ ,$$

$$M_2(N,p) = \frac{(e^{\rho N} - 1)^2}{(\rho N)^2 e^{2\rho N}} \ ; \quad \rho = \ln(1+p) \ , \tag{E3}$$

from (9.11a) . Performing the indicated differentiation (E1), we find that

$$e^{\rho N}(a\rho + b) = 2a\rho + b \tag{E4}$$

where

$$a = N(2 - k(N-1)^2) \ ; \quad b = 2 + k(N-1) \ . \tag{E5}$$

To find a value of ρ which is maximum at some value of N, we must solve the transcendental equation,

$$e^{\rho N} = \frac{a\rho}{a\rho + b} + 1 \ . \tag{E6}$$

Since most of the intersections of these two lines are very close to

$\rho = 0$, an approximation may be used for $e^{\rho N}$, viz.:

$$e^{\rho N} = 1 + \rho N + \frac{(\rho N)^2}{2} ,$$

so that on solving for ρ we obtain the quadratic equation

$$[\frac{N^2 a}{2}] \rho^2 + N[N\frac{b}{2} + a]\rho + [Nb - a] = 0 . \qquad (E7)$$

The solution of this equation is

$$\rho = \ln(1+p) \doteq p = -\frac{B}{2A} + [\frac{B}{2A} - \frac{A}{C}]^{1/2} , \qquad (E8)$$

$$\frac{B}{2A} = \frac{3 - C(1-N)(3/2 - N)}{N[2 - C(1-N)^2]} ; \quad [-\frac{A}{C}] = \frac{2C(1-N)}{N[2 - C(1-N)^2]} .$$

For the ranges of interest, this may be written as

$$p \doteq -\frac{B}{A} + (\frac{B}{A}) + \frac{1}{2}(-\frac{C}{A})(\frac{B}{A})^{-1}$$

by the binomial theorem, and

$$p \doteq -\frac{1}{2}\frac{C}{B} = \frac{2k(1-N)}{[3 - k(1-N)(\frac{3}{2} - N)]} . \qquad (E9)$$

The expression (E9) was used in obtaining Fig. 29. The expression can, of course, be more accurately represented by replacing ρ by $\log(1+p)$.

APPENDIX F

The Calculation of G'(p) for Small Input s/n

Only one term of G'(p) is calculated here: $g_0'(v)$. Setting ${}_1F_1 = 1$ in the expression for C_{mn} (10.5), we obtain, for $p \ll 1$, $K = 1$,

$$C_{mn}/C_{\nu} \cong \left[\frac{\epsilon_m}{(m!)^2} P^m\right]\left[\frac{2^n}{n!}\right]\left[\omega_F T_{mn}\right]\left[\frac{\Gamma(\frac{\nu}{2}+1)}{\Gamma(\frac{\nu}{2}+1-\ell)}\right]^2 \qquad (F1)$$

Here $g'_o(\nu)$ corresponds to the term of (F1) for which m=0, so that

$$g'_o(\nu) = \sum_{k=1} \left[\frac{2^{2k}}{(2k)!}\right]\left[\omega_F T_{0,2k}\right]\left[\frac{\Gamma(\frac{\nu}{2}+1)}{\Gamma(\frac{\nu}{2}+1-k)}\right]^2 , \qquad (F2)$$

where we have set $2\ell = n = 2k$.

From (6.14) we have

$$\frac{2^{2k}}{(2k)!} = \frac{1}{(\frac{1}{2})_k\, k!}$$

and from the definition of $(a)_k$, we can accordingly write

$$\left[\Gamma(\tfrac{\nu}{2}+1)/\Gamma(\tfrac{\nu}{2}+1-k)\right]^2 = (\tfrac{\nu}{2}+1-k)_k^2 = (-\tfrac{\nu}{2})_k^2 \qquad (F3)$$

Hence, we have

$$g'_o(\nu) = \sum_{k=1} \frac{(-\frac{\nu}{2})_k^2}{k!\,(\frac{1}{2})_k}\left(\omega_F T_{0,2k}\right) \qquad (F4)$$

APPENDIX G

The Calculation of $(F_{s+n})_{B.B.}$ for Strong Signals: Broad-band Noise, with a General Spectral Shape

Using the same assymptotic form for ${}_1F_1$ as in Appendix D, since S, the signal increment, is independent of the signal band structure, we have:

$$N = \nu/2 \tag{G1}$$

$$H(p) \equiv \frac{p^{2N}}{\Gamma(N+1)^2} \; Z(N,p) \tag{G2}$$

where $Z(N,p) = L(N)^2 + N^2 L(N)\, p^{-1} + [N^2(N+1)^2 L(N) + N^4]\, p^{-2}$ (G3)

and

$$L(N) = [1 + \Gamma(N+1)\, p^{-N}] \tag{G4}$$

However, the denominator G'(p) is (10.14)

$$G'(p) \sum_{\substack{\ell=1 \\ m+n \neq 2\ell}}^{\infty} \frac{C_{mn}}{C_\nu} \; (\omega_F T_{mn}) \tag{G5}$$

where now, $\frac{\Gamma(N+1)^2}{p^{2N}} \; \frac{C_{mn}}{C_\nu} = \epsilon_m [p^{-n} \; \frac{2^n}{n!}] [(-\frac{\nu}{2})_\ell \; (-\frac{\nu}{2})_{\ell - m}]^2 g_{mn}(p)$ (G6)

where

$$g_{mn}(p) = 1 + 2(N-\ell)(N+m-\ell)\, p^{-1} \tag{G7}$$

$$+ (N-\ell)(N+m-\ell)[2(N-\ell)(N+m-\ell+1)$$

$$-4(N-\ell) - m + 1]\, p^{-2} \tag{G7}$$

Hence we write

$$\left(\frac{2}{\pi}\frac{\omega_P}{\omega_F}\right) P_{s+n} \simeq \frac{p\,Z(N,p)}{\sum_{\substack{\ell_i=1 \\ 2\ell=m+n}} \epsilon_m p^{-n+1} \left[\frac{2^n}{n!}\right] \left[(-N)_{\ell}(-N)_{\ell-m}\right]^2 (\omega_F T_{mn}) g_{mn}(p)} \qquad \text{(G8)}$$

Collecting terms from g_{11}, g_{02}, g_{22}, g_{13}, and g_{33}, we obtain

$$\left(\frac{2}{\pi}\frac{\omega_P}{\omega_F}\right) P_{s+n} = \frac{p}{4N^2}\left[A_o + A_1 p^{-1} + A_2 p^{-2}\right] \qquad \text{(G9)}$$

$$A_o = (\omega_F T_{11})$$

$$\frac{A_1}{\omega_F} = 2N(N-1)\,T_{11} + \frac{N^2}{2} T_{02} + (N-1)^2 T_{22}$$

$$\frac{A_2}{\omega_F} = 2(N-1)^2\left[N(N-1)\,T_{11} + \frac{N^2}{2} T_{02} + \frac{N(N-2)}{2} T_{22}\right.$$

$$\left. + \frac{1}{3} N^2 T_{13} + \frac{1}{3}(N-2)^2 T_{33}\right] \qquad \text{(G10)}$$

For the ideal clipper, as in Appendix D,

$$\lim_{N\to 0} \frac{L(N)^2}{N^2} = (\ln p + \gamma)^2 \quad , \quad \gamma = 0.5772\cdots \quad , \quad \text{Euler's number;}$$

for $\nu = 0$, then

$$\left(\frac{2}{\pi}\frac{\omega_P}{\omega_F}\right) P_{s+n} \simeq p(\ln p + \gamma)^2/4\left[A_o + A_1 p^{-1} + A_2 p^{-2}\right] \qquad \text{(G11)}$$

$$\simeq p\,(\ln p + \gamma)^2/4\, A_o \quad . \qquad \text{(G12)}$$

REFERENCES

1. J. H. Van Vleck and D. Middleton, J. Appl. Phys. 17, 940 (1946).
2. B. Dwork, Proc. I. R. E. 39, 771 (1950).
3. T. S. George, Proc. Inst. Elect. Eng., (London) IV 99, 92 (Feb. 1952).
4. L. A. Zadeh and J. R. Ragazzini, Proc. I.R.E. 40, 1223 (1952).
5. D. Middleton, Quart. Appl. Math. 5, 445 (1948). W. B. Davenport, R. A. Johnson, D. Middleton, A. Appl. Phys. 23, 377 (1952). D. Middleton, The Statistical Theory of Signal Detection, I. Optimum Detection of Signals in Noise. Lincoln Laboratory Report No. T. R. 35, (1953); J. Appl. Phys. 24, 371 (1953); Proc. I. R. E. 36, 1467 (1948).
6. N. Wiener, Acta Math. 55, 117 (1930).
7. A. Khintchine, Math. Ann. 109, 604 (1934).
8. J. L. Lawson and G. E. Uhlenbeck, Threshold Signals, Radiation Laboratory Service 24, McGraw-Hill, New York, 1950.
9. D. Middleton, J. Appl. Phys. 24, 371 (1953).
10. N. Wiener, Extrapolation, Interpolation, and Smoothing of Stationary Time Series, John Wiley, N. T., 1950.
11. The Staff of the Computation Laboratory, Tables of the Error Function and of Its First Twenty Derivatives, Harvard University Press, Cambridge, Massachusetts, 1952.
12. H. Cramér, Mathematical Methods of Statistics, Princeton University Press, 1951. S. O. Rice, Bell Syst. Tech. J. 23, 282 (1944); 24, 46 (1945).
13. J. J. Faran and Robert Hills, Correlators for Signal Reception, Technical Memorandum No. 27, Acoustics Research Laboratory, Harvard University, Cambridge, Massachusetts, September 15, 1952. Carl Eckart, The Measurement and Detection of Steady A. C. and D. C. Signals in Noise, University of California Marine Physics Laboratory of Scripps Institute of Oceanography, Ref. 51-39, October 4, 1951.

DISTRIBUTION LIST

Technical Reports

2	Chief of Naval Research (427) Department of the Navy Washington 25, D. C.
1	Chief of Naval Research(460) Department of the Navy Washington 25, D. C.
1	Chief of Naval Research (421) Department of the Navy Washington 25, D. C.
6	Director (Code 2000) Naval Research Laboratory Washington 25, D. C.
2	Commanding Officer Office of Naval Research Branch Office 150 Causeway Street Boston, Massachusetts
1	Commanding Officer Office of Naval Research Branch Office 1000 Geary Street San Francisco 9, California
1	Commanding Officer Office of Naval Research Branch Office 1030 E. Green Street Pasadena, California
1	Commanding Officer Office of Naval Research Branch Office The John Crerar Library Building 86 East Randolph Street Chicago 1, Illinois
1	Commanding Officer Office of Naval Research Branch Office 346 Broadway New York 13, New York
3	Officer-in-Charge Office of Naval Research Navy No. 100 Fleet Post Office New York, N. Y.

1	Chief, Bureau of Ordnance (Re4) Navy Department Washington 25, D. C.
1	Chief, Bureau of Ordnance (AD-3) Navy Department Washington 25, D. C.
1	Chief, Bureau of Aeronautics (EL-1) Navy Department Washington 25, D. C.
2	Chief, Bureau of Ships (810) Navy Department Washington 25, D. C.
1	Chief of Naval Operations (Op-413) Navy Department Washington 25, D. C.
1	Chief of Naval Operations (Op-20) Navy Department Washington 25, D. C.
1	Chief of Naval Operations (Op-32) Navy Department Washington 25, D. C.
1	Director Naval Ordnance Laboratory White Oak, Maryland
2	Commander U. S. Naval Electronics Laboratory San Diego, California
1	Commander (AAEL) Naval Air Development Center Johnsville, Pennsylvania
1	Librarian U. S. Naval Post Graduate School Monterey, California
50	Director Signal Corps Engineering Laboratories Evans Signal Laboratory Supply Receiving Section Building No. 42 Belmar, New Jersey

3	Commanding General (RDRRP) Air Research and Development Command Post Office Box 1395 Baltimore 3, Maryland
2	Commanding General (RDDDE) Air Research and Development Command Post Office Box 1395 Baltimore 3, Maryland
1	Commanding General (WCRR) Wright Air Development Center Wright-Patterson Air Force Base, Ohio
1	Commanding General (WCRRH) Wright Air Development Center Wright-Patterson Air Force Base, Ohio
1	Commanding General (WCRE) Wright Air Development Center Wright-Patterson Air Force Base, Ohio
2	Commanding General (WCRET) Wright Air Development Center Wright-Patterson Air Force Base, Ohio
1	Commanding General (WCREO) Wright Air Development Center Wright-Patterson Air Force Base, Ohio
2	Commanding General (WCLR) Wright Air Development Center Wright-Patterson Air Force Base, Ohio
1	Commanding General (WCLRR) Wright Air Development Center Wright-Patterson Air Force Base, Ohio
2	Technical Library Commanding General Wright Air Development Center Wright-Patterson Air Force Base, Ohio
1	Commanding General (RCREC-4C) Rome Air Development Center Griffiss Air Force Base Rome, New York
1	Commanding General (RCR) Rome Air Development Center Griffiss Air Force Base Rome, New York

2	Commanding General (RCRW) Rome Air Development Center Griffiss Air Force Base Rome, New York
6	Commanding General (CRR) Air Force Cambridge Research Center 230 Albany Street Cambridge 39, Massachusetts
1	Commanding General Technical Library Air Force Cambridge Research Center 230 Albany Street Cambridge 39, Massachusetts
2	Director Air University Library Maxwell Air Force Base, Alabama
1	Commander Patrick Air Force Base Cocoa, Florida
2	Chief, Western Division Air Research and Development Command P. O. Box 2035 Pasadena, California
1	Chief, European Office Air Research and Development Command Shell Building 60 Rue Ravenstein Brussels, Belgium
1	U. S. Coast Guard (EEE) 1300 E Street, N. W Washington, D. C.
1	Assistant Secretary of Defense (Research and Development) Research and Development Board Department of Defense Washington 25, D. C.
5	Armed Services Technical Information Agency Document Service Center Knott Building Dayton 2, Ohio

1	Director Division 14, Librarian National Bureau of Standards Connecticut Avenue and Van Ness St., N. W.
1	Director Division 14, Librarian National Bureau of Standards Connecticut Avenue and Van Ness St., N. W.
1	Office of Technical Services Department of Commerce Washington 25, D. C.
1	Commanding Officer and Director U. S. Underwater Sound Laboratory New London, Connecticut
1	Federal Telecommunications Laboratories, Inc. Technical Library 500 Washington Avenue Nutley, New Jersey
1	Librarian Radio Corporation of America RCA Laboratories Princeton, New Jersey
1	Sperry Gyroscope Company Engineering Librarian Great Neck, L. I., New York
1	Watson Laboratories Library Red Bank, New Jersey
1	Professor E. Weber Polytechnic Institute of Brooklyn 99 Livingston Street Brooklyn 2, New York
1	University of California Department of Electrical Engineering Berkeley, California
1	Dr. E. T. Booth Hudson Laboratories 145 Palisade Street Dobbs Ferry, New York
1	Cornell University Department of Electrical Engineering Ithaca, New York

1	University of Illinois Department of Electrical Engineering Urbana, Illinois
1	Johns Hopkins University Applied Physics Laboratory Silver Spring, Maryland
1	Professor A. von Hippel Massachusetts Institute of Technology Research Laboratory for Insulation Research Cambridge, Massachusetts
1	Director Lincoln Laboratory Massachusetts Institute of Technology Cambridge 39, Massachusetts
1	Signal Corps Liaison Office Massachusetts Institute of Technology Cambridge 39, Massachusetts
1	Mr. Hewitt Massachusetts Institute of Technology Document Room Research Laboratory of Electronics Cambridge, Massachusetts
1	Stanford University Electronics Research Laboratory Stanford, California
1	Professor A. W. Straiton University of Texas Department of Electrical Engineering Austin 12, Texas
1	Yale University Department of Electrical Engineering New Haven, Connecticut
1	Mr. James F. Troccn, Administrative Aide Columbia Radiation Laboratory Columbia University 538 West 120th Street New York 27, N. Y.
1	Dr. J.V.N. Granger Stanford Research Institute Stanford, California